Environment Canada Environnement Canada

Canada

Valley Cold Pools in GEM

R. McTaggart-Cowan, M. Desgagne, M. Faucher, C. Girard and A. Zadra

RPN-A

v1.0

2 January 2013

Contents

- Description of valley cold pools (VCPs)
  - VCP background and physics
  - Over-cooling of VCPs in GEM
- Root cause analysis of over-cooling
  - Description of the diagnostic testbed
  - Problem simplification and analysis of 1D advection
  - “Proof of concept” adjustment to eliminate over-cooling
- Development of a conceptual model of over-cooling
  - Required ingredients and setup for the VCP over-cooling feedback
  - Step-by-step description of an event
- Consideration of other VCP error sources
- Effect of a proposed solution on simulations and scores
- Discussion of alternative solutions to prevent VCP over-cooling

Goals of the Presentation

- The investigation described here has been undertaken in the last three weeks: this presentation is an update on the error analysis, since it may have implications for all GEM-based modelling systems
- The goals of this presentation are:
  - to provide a distinction between real VCPs and the VCP over-cooling pathology identified in GEM
  - to present a compelling case for the fact that we understand the origins of VCP over-cooling in GEM
  - to propose a solution that effectively eliminates the over-cooling process without adversely affecting guidance in general
  - to demonstrate the efficacy and side-effects of this solution
  - to initiate a discussion on other possible solutions

The VCP as a Real Feature

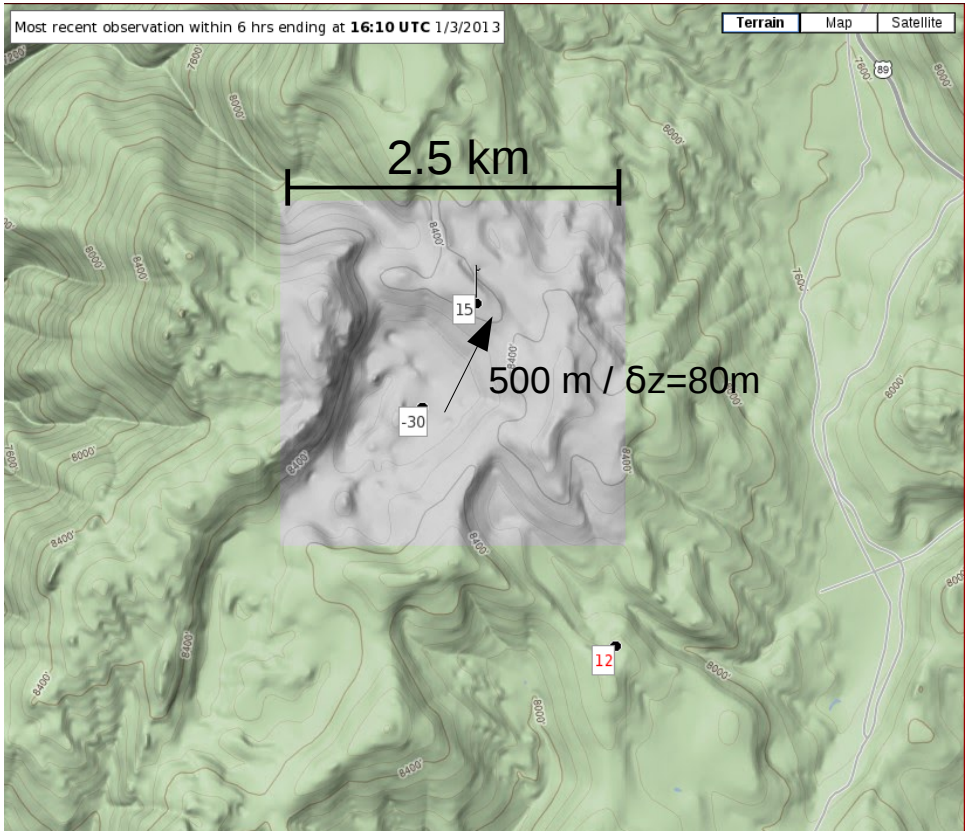

Surface temperature observations (Farenheit: -30°F = -24°C; 15°F = -9°C) from the Utah mesonet for 1600 UTC 3 January 2013, near Peter Sinks. (Courtesy of Trevor Alcott, NOAA/NWS)

- Valley cold pools are features observed in nature
- VCPs are small-scale structures in both the horizontal and vertical
- Even within the model environment, not all cold air in a valley aresult of the over-cooling mechanism to be described here: many physical processes can lead to the formation of very cold VCPs

Description of VCP Structure

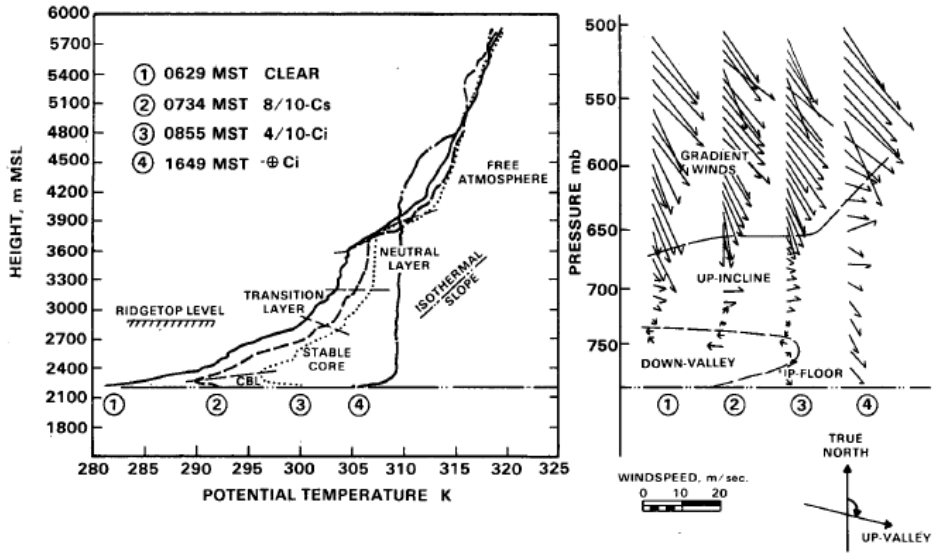

Profile 1 (solid line in left panel) shows a 20 K VCP inversion below ridge level, with clear separation of the flow below the inversion top (675 mb).

Tethersonde observations at Eagle Valley for 13-14 October 1978 (from Whiteman 1982).

- In addition to overnight temperature and wind forecasts, VCPs affect local predictions of:
  - precipitation type/phase
  - fog, visibility and icing conditions
  - air quality

Description of VCP Destruction

VCP inversion fills the valley before sunrise

Surface heating (insolation) leads to the development of a shallow convective boundary layer (CBL)

CBL deepening slows as energy is converted into buoyancy-driven upslope flows; mid-valley subsidence is required by continuity

Remnant VCP core warms as it sinks towards the valley floor

CBL dominates as the VCP inversion is eliminated

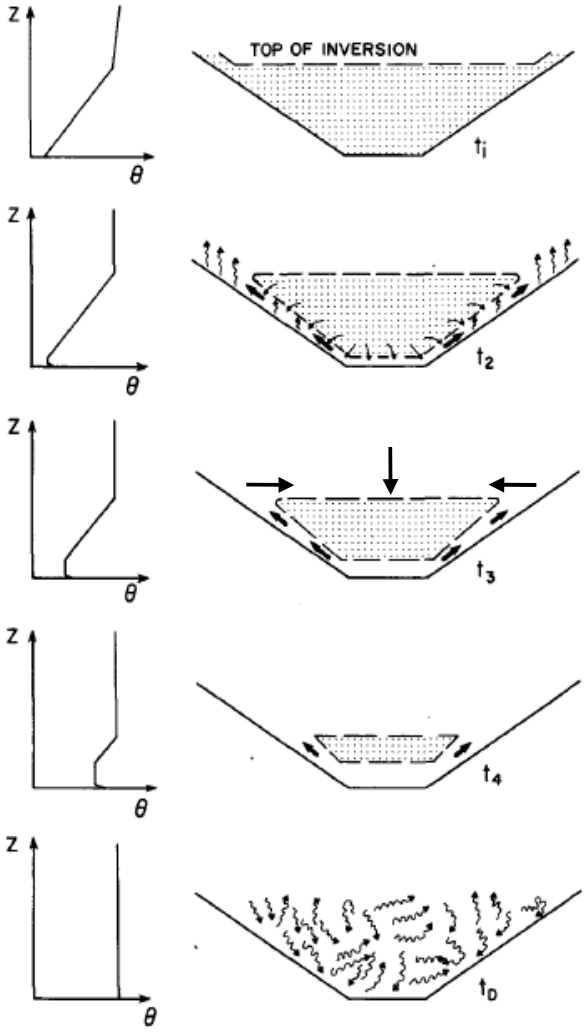

Conceptual model of VCP breakup after sunrise (t_i-t_2) presented by Whiteman (1982).

Description of VCPs in NWP

- NWP performance is generally poor for VCPs (Hart et al. 2004)
  - Near-surface temperature is generally not cold enough (inversion is too weak)
  - VCP breakdown is generally predicted too early
- Forecaster feedback on the 2.5 km and 1 km systems used during the 2010 Olympics suggests that GEM produces VCP guidance of generally acceptable quality
- However, during the development of the 1 km configuration, over-cooling in a VCP led to near-surface temperatures below -100^{o}C, which caused GEM to abort

History of VCPs in GEM (Olympics)

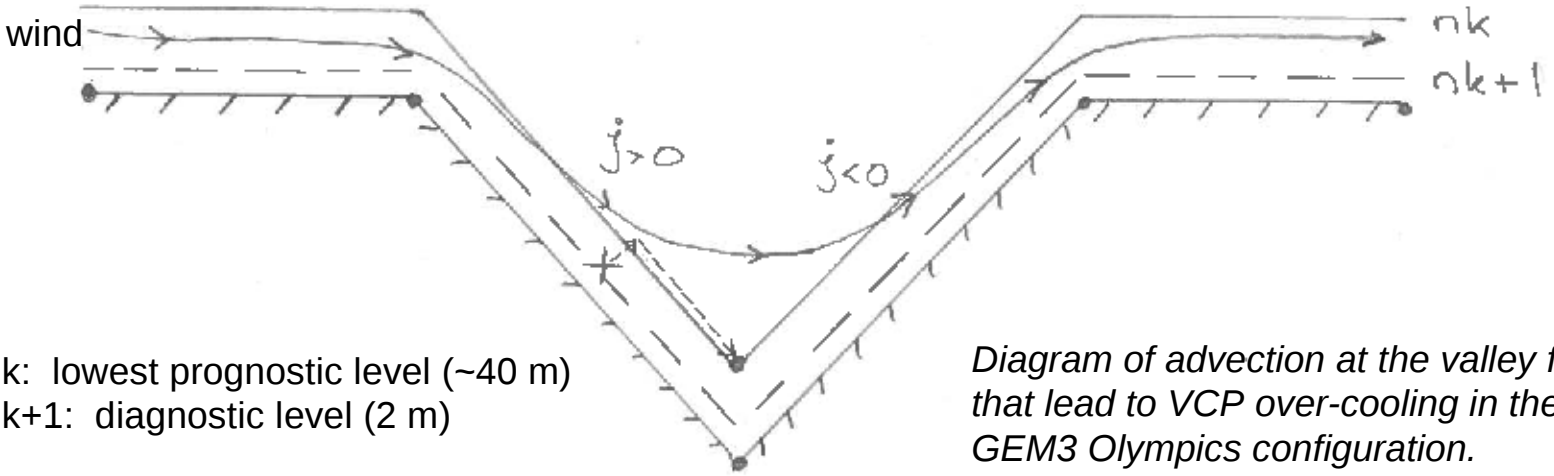

nk: lowest prognostic level (~40 m)
nk+1: diagnostic level (2 m)

Diagram of advection at the valley floor that lead to VCP over-cooling in the GEM3 Olympics configuration.

- Moderately strong cross-valley winds ride over the VCP
- A dipole of “zeta-dot” (vertical displacement in the model coordinate) develops across the valley
- In the downslope region, GEM3 uses the diagnostic level to interpolate vertically to the upwind point, which lies below the lowest prognostic level

History of VCPs in GEM (Olympics)

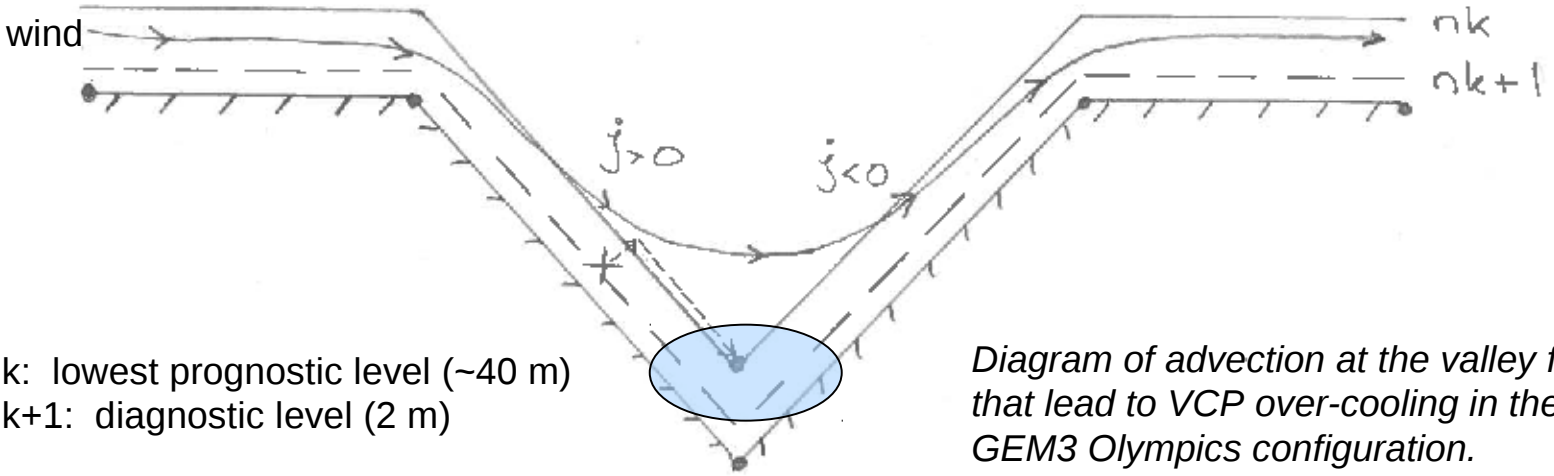

nk: lowest prognostic level (~40 m)
nk+1: diagnostic level (2 m)

Diagram of advection at the valley floor that lead to VCP over-cooling in the GEM3 Olympics configuration.

- The cold air in the inversion parameterized by the stability functions is “dug out” by GEM3 advection
- This leads to a cycle of cooling because of the mix of resolved (advective) and parameterized states
- This problem is resolved in GEM4, where the model dynamics does not consider the diagnostic level

History of VCPs in GEM (Strato)

Background

Small-scale oscillations were identified during the development of the “Strato-3” GDPS, particularly along the coast of Antarctica. 2δt oscillations triggered by such fields led to a model failure in a Strato-3 cycle.

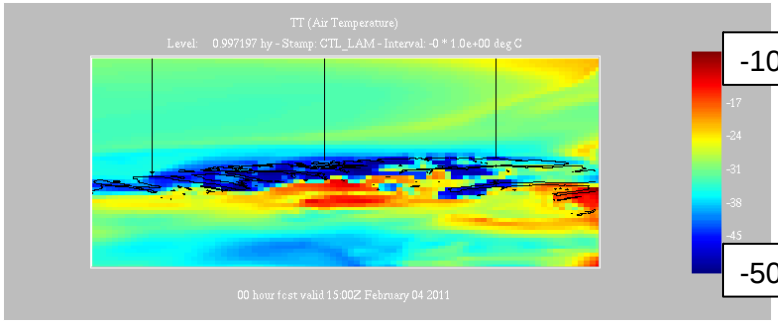

Lowest-level temperature in a GDPS-based LAM grid.

Advecting winds (3D) are computed within the C-N step as:

$$V_{adv} = \frac{1}{2} (V^{-} + V^{*})$$

Winds from the previous step (V^{-}) have been smoothed by diffusion, while those at the current step (V^{*}) have not: inconsistent spatial scales

Diffusing the vertical component (zeta-dot) within the C-N (Schm_hzdzdt_L = .true.) eliminates the observed oscillations.

History of VCPs in GEM (Strato)

- The application of horizontal diffusion on only the vertical component of the advecting wind leads to another over-cooling error, this time in the GDPS
- To eliminate this diffusion-induced inconsistency, all three V* wind components are diffused simultaneously for the C-N steps (Schm_hzdzdt_L=.true., Schm_hzduav_L=.true.)

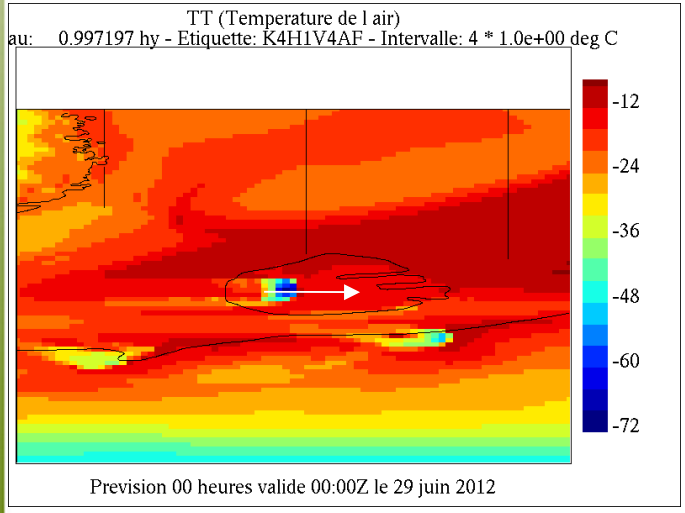

Lowest-level temperature in the GDPS, over Berkner Island near Antarctica.

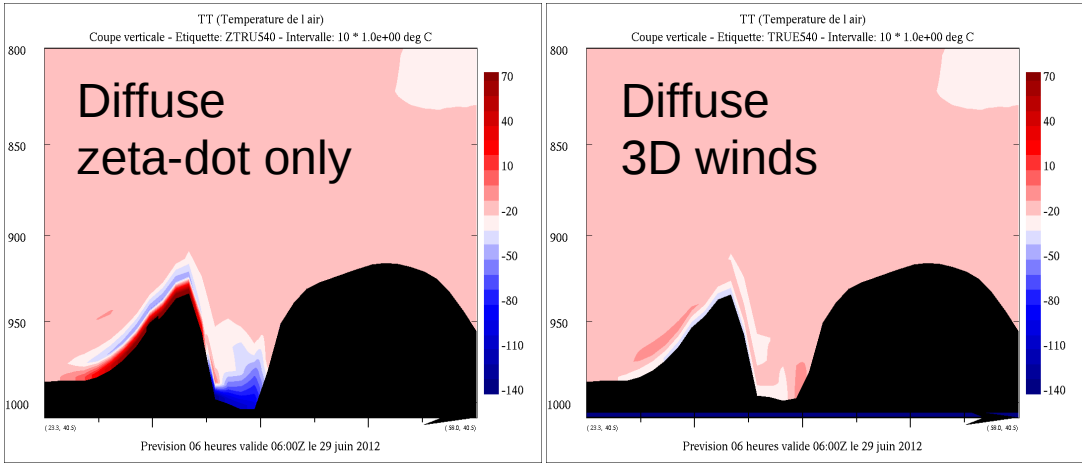

Zonal cross section of temperature through the VCP temperature minimum for two different C-N diffusion strategies

Recent VCP Problems in GEM

- More recently, the HRDPS experienced a large number of model failures (5 / 14 integrations) with the National 2.5 km grid

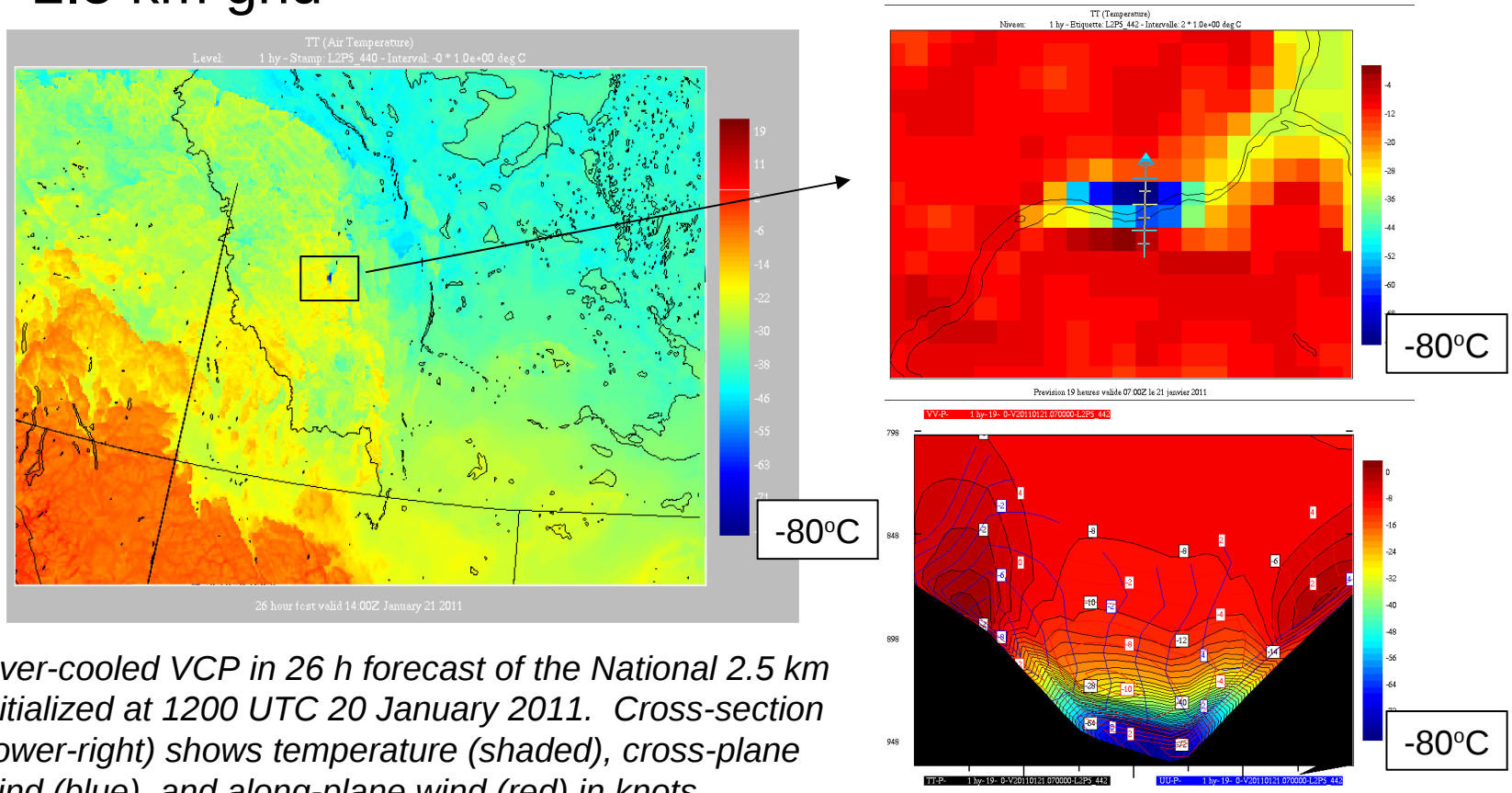

Over-cooled VCP in 26 h forecast of the National 2.5 km initialized at 1200 UTC 20 January 2011. Cross-section (lower-right) shows temperature (shaded), cross-plane wind (blue), and along-plane wind (red) in knots.

Recent VCP Problems in GEM

- Several approaches failed to eliminate the problem completely:
  - Use of filtered topography to eliminate $2\Delta x$ mountains
  - Use of dynamic roughness length instead of vegetation-only values
  - Increasing the value of the horizontal diffusion coefficient (from ∇^4 0.2 to ∇^4 0.4)
  - Adding horizontal diffusion to the current time-level winds in the Crank-Nicholson iterations
- The final two adjustments were found to limit the over-cooling sufficiently to produce a physically reasonable result for the case studied; however, they do not prevent over-cooling in all cases

Recent VCP Problems in GEM

- Despite the use of C-N diffusion, a “perpetual January” run of the YEC-15 GDPS (Yin-Yang grid) aborted with another over-cooling error just before Christmas
- The operational West and Arctic HRDPS windows have aborted with an over-cooling error three times in the last month

Pathological VCP over-cooling has now proved fatal in at least three upcoming and operational configurations. A full evaluation of the problem and a solution are required.

VCP Over-Cooling: Starting Point

- VCP over-cooling leads to lower-level temperatures less than -100^{o}C before the model aborts, typically in the thermodynamic functions that are (understandably) not designed for such temperatures
- Since VCP over-cooling leads to a high-stability state, it is possible that more than one error source could lead to a similar symptom (several sources have already been identified over the last couple of years)
- The error must be locally systematic, but is not necessarily one-signed everywhere since a heating error would not cause any numerical problems due to buoyancy

VCP Over-Cooling Morphology

1) VCP over-cooling occurs in basins (3D bowls) within narrow valleys. These valleys appear to be on the order of 4-10 gridpoints wide (from peak to peak), with resolved slopes that are not unreasonably steep (on the order of 100 m km^{-1}).

Lake Baikal, Siberia

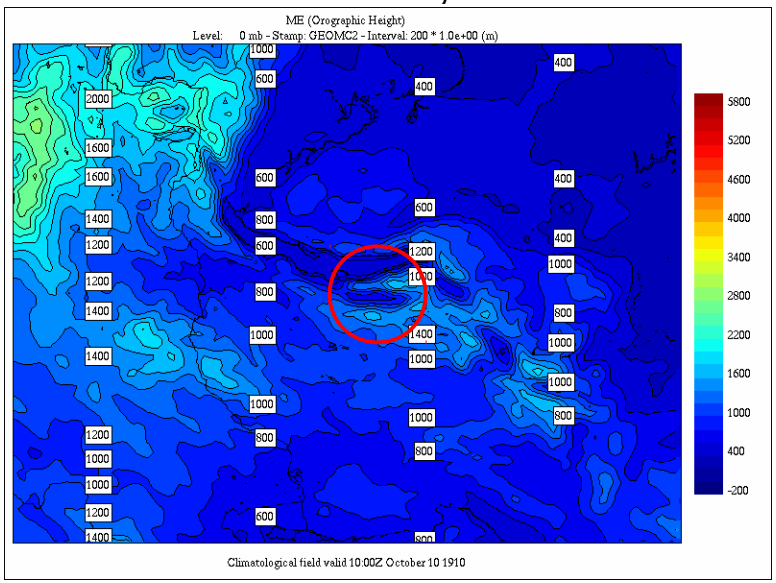

Mackenzie Mountains, NWT

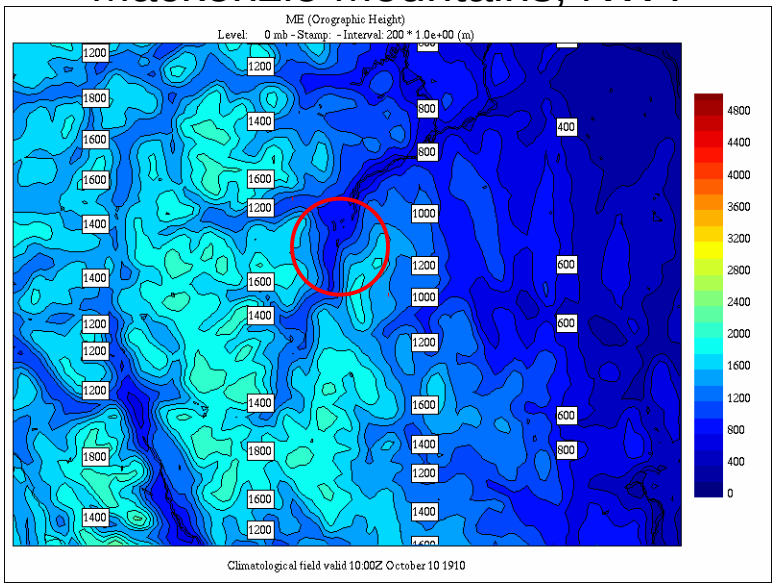

Orographic fields (shaded at 200 m intervals) of GDPS (left) and national HRDPS (right) simulations that led to over-cooling errors. The locations of the events are identified with a red circle on each panel.

VCP Over-Cooling Morphology

2) Events occur over a period of hours to days, and are associated with sustained cooling rates between 10 K d^{-1} and 150 K d^{-1} in the near-surface layers. Note that an aborted over-cooling event occurs earlier in the GDPS configuration (blue arrow in the left panel).

Lake Baikal, Siberia

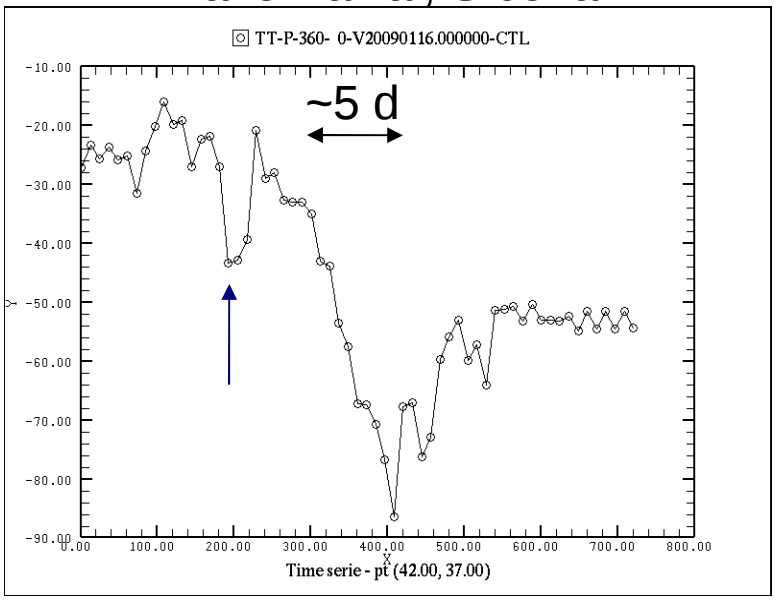

Mackenzie Mountains, NWT

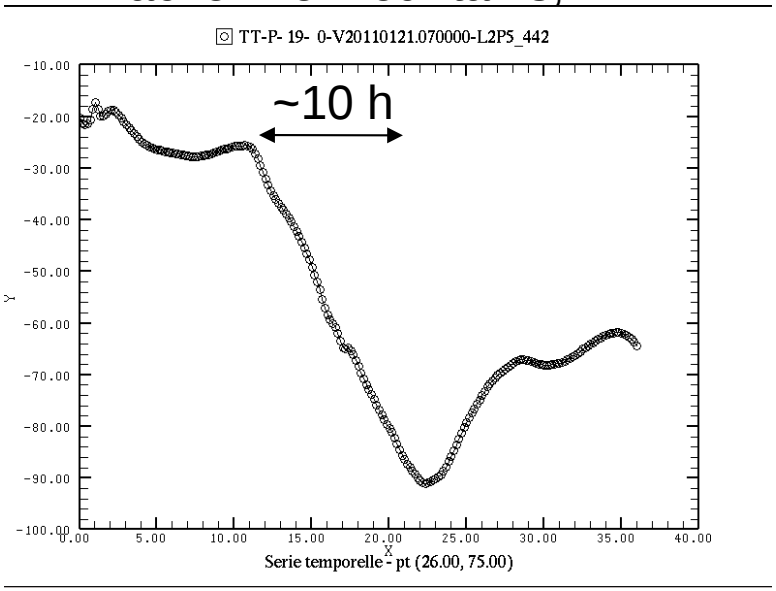

Time series of lowest-level (~20 m) temperatures in the GDPS (left) and national HRDPS (right) configurations that led to over-cooling errors. Outputs are produced at 12-hourly intervals for the GDPS and at each timestep (60s) in the HRDPS.

VCP Over-Cooling Morphology

3) VCP over-cooling occurs across a range of configurations and physics options. This has been confirmed by a number of tests involving modified and reduced physics options.

GDPS YEC-15 Configuration

Parameter	Value
Grid spacing	~15 km
Configuration	Yin-Yan
Time step	450 s

Process	Scheme
PBL	CLEF
Gridscale	Sunqvist
CPS	Fritsch-Chappell
Radiation	CCCma
Surface	ISBA

HRDPS National Configuration

Parameter	Value
Grid spacing	2.5 km
Configuration	LAM
Time step	60 s

Process	Scheme
PBL	Moistke
Gridscale	Milbrandt-Yau 2M
CPS	None
Radiation	CCCma
Surface	ISBA

VCP Over-Cooling Case Selection

- A test grid is developed to focus on the GDPS “perpetual winter” run failure over the Lake Baikal region
- The 45x55 gridpoint co-aligned domain is nested at each timestep from the driving global YEC-15 model
- Not a pure “acid test” because of round-off errors, but the mid-month VCP overcooling is reproduced

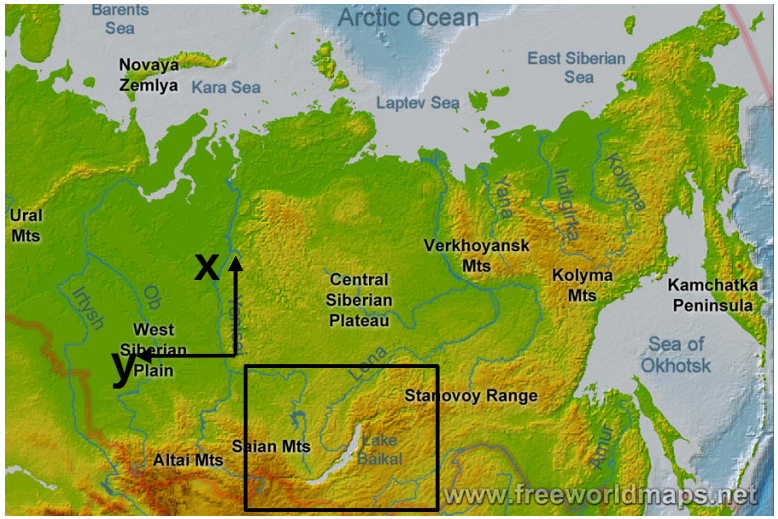

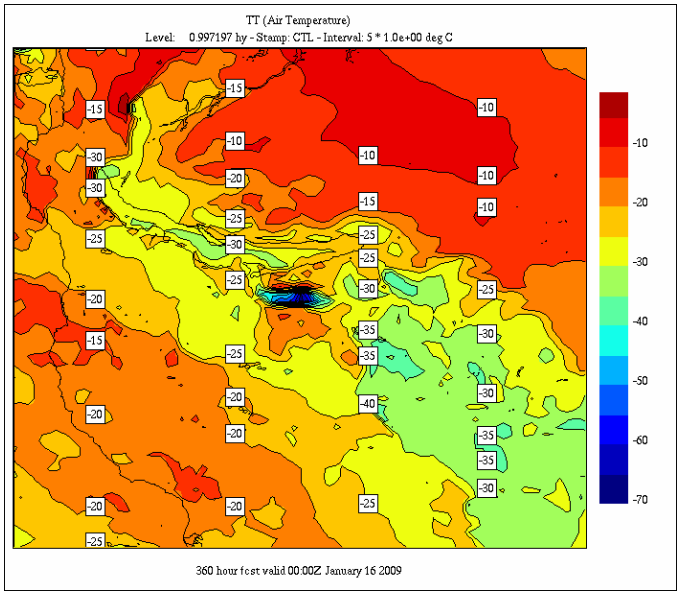

Position/orientation (left) and day-16 lowest-level temperature (right) on the GDPS test grid.

Root Cause Analysis of Error

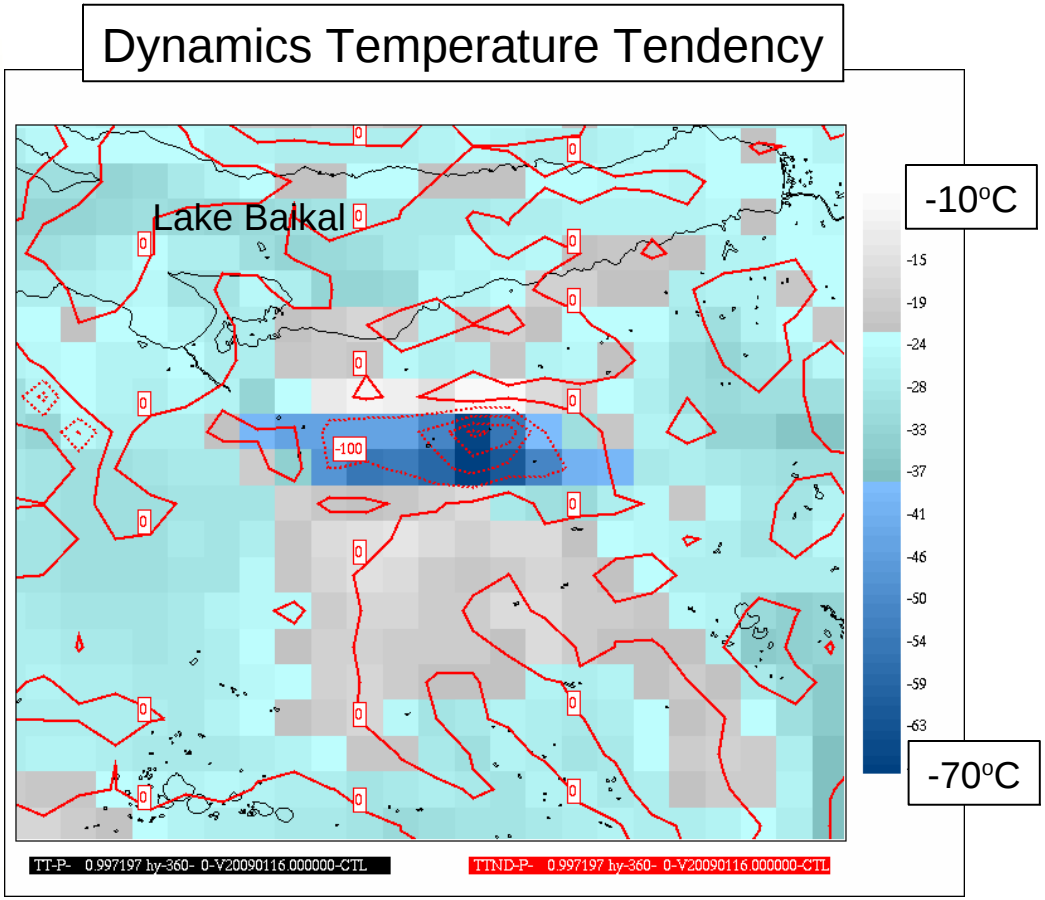

Lowest-level temperature (shaded in °C as indicated on the color bar) and instantaneous temperature tendency from the dynamics (TTND, in red contours at intervals of 100 K d^{-1}) after 360 h of integration on the GDPS test grid.

The coldest point in the temperature field is co-located with the maximum negative tendency from the dynamics.

The unphysically-large (-400 K d^{-1}) cooling rate further suggests that the dynamics are responsible for VCP over-cooling in this case.

The physics is able to offset much of this cooling, but eventually the ground temperature drops and surface fluxes cannot sufficiently heat the overlying air.

Root Cause Analysis of Error

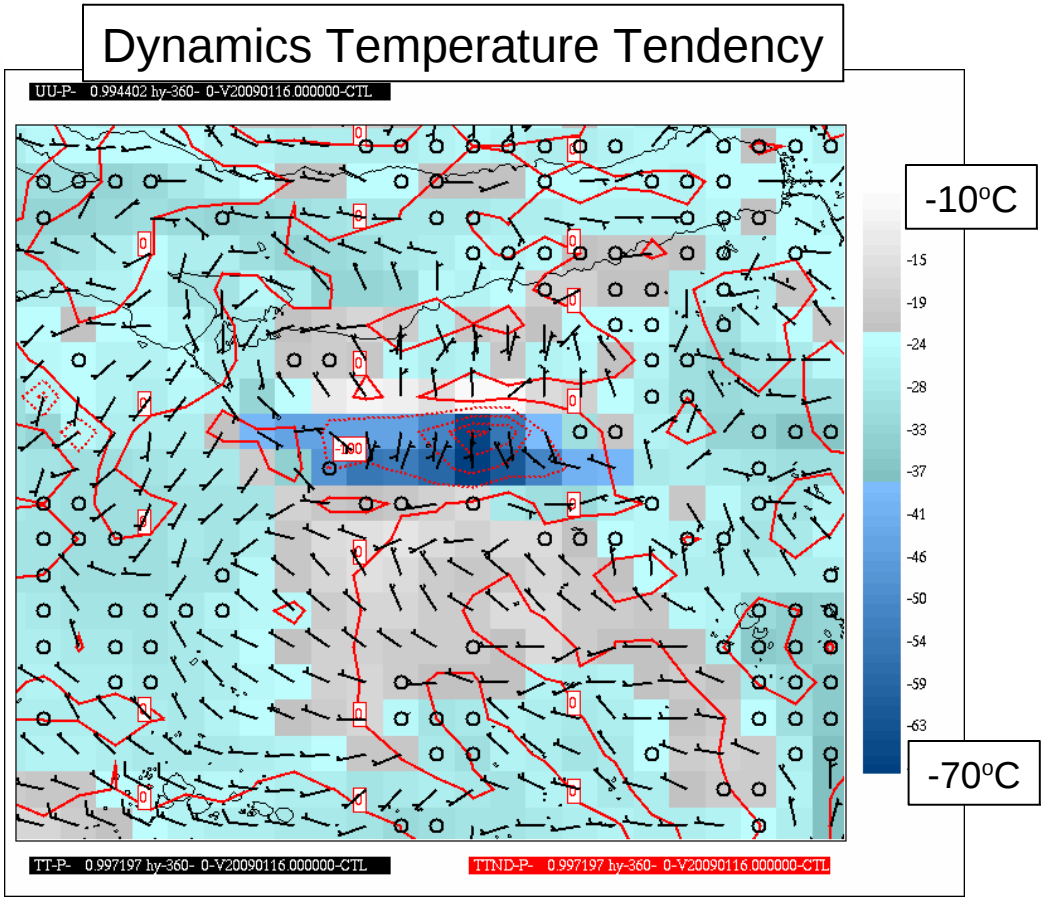

Lowest-level temperature (shaded in °C as indicated on the color bar), instantaneous temperature tendency from the dynamics (TTND, in red contours at intervals of 100 K d^{-1}) and lowest-level winds (wind barbs in knots).

As in observed VCPs, the flow within the cold layer is isolated from the surrounding flow due to the strong static stability.

In this case, air diverges from the axis of the VCP such that the air at both of the coldest points is advected from within the cold pool itself.

This structure may allow for a reduction of the advection problem to 1D, since vertical motions are weak at the lowest model level.

Root Cause Analysis of Error

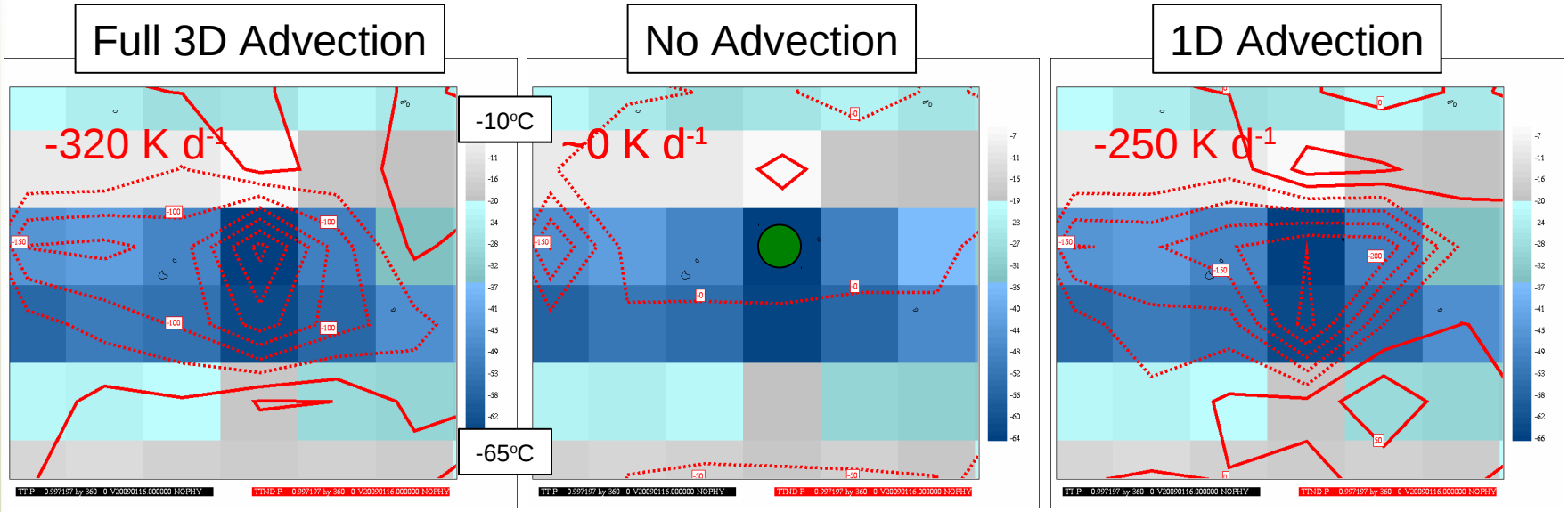

Lowest-level temperature (shaded in ºC as indicated on the color bar) and instantaneous temperature tendency from the dynamics (TTND, in red contours at intervals of 50 K d^{-1}) after a single timestep at 360 h of integration on the GDPS test grid. The coldest point is shown with a green dot.

Problem size is reduced to a 3x3 grid point configuration centered on the area of maximum cooling, run for a single time step.

Solver and diffusion (non-advective dynamics) tendency is near-zero in the region of interest.

Reduction of advection problem to 1D (v-component advecting wind only) reproduces 80% of the original tendency signal.

Root Cause Analysis of Error

Semi-Lagrangian Advection

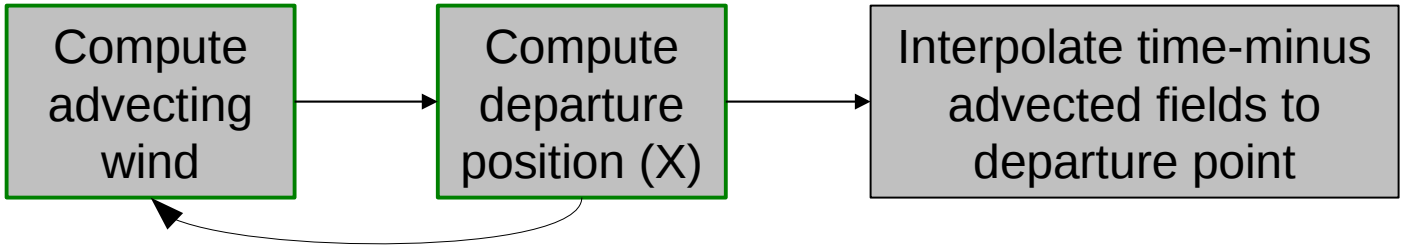

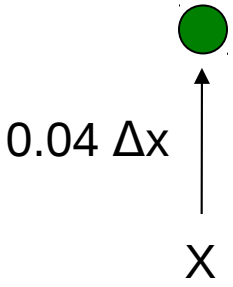

The positive V-wind at the coldest point means that the computed departure point is in the negative y-direction on the model grid. Light winds mean that the distance to the departure point is only 4% of the distance to the next upwind gridpoint.

This departure position is confirmed analytically for this simplified setup using a prescribed 1D wind value.

This confirms the correct functioning of the first two steps in this case.

Root Cause Analysis of Error

Semi-Lagrangian Advection

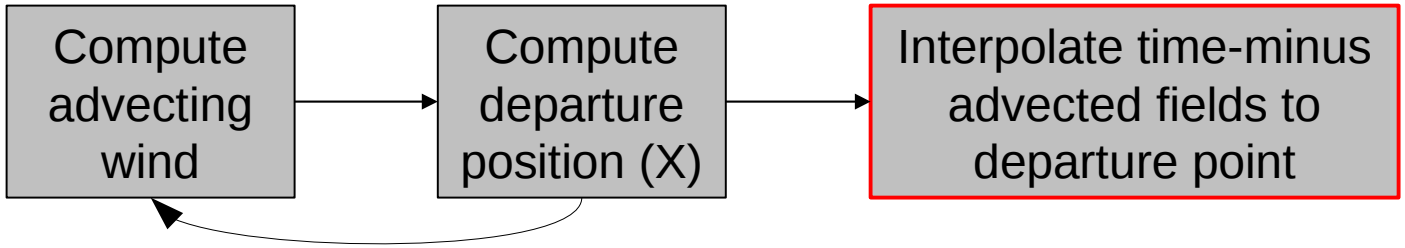

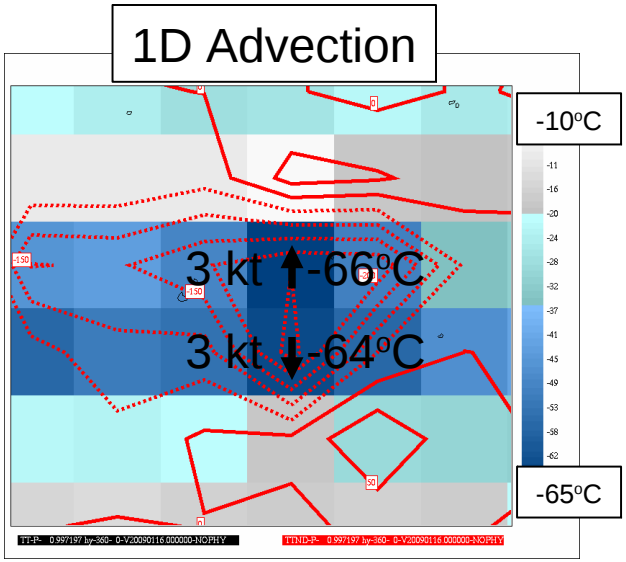

Since it is the advective component of the dynamics tendency that is unphysically negative in this case, it appears that the VCP overcooling is a result of interpolation to the departure point.

The advection problem is further simplified by considering the coldest point in isolation.

Lowest-level temperature (shaded in °C as indicated on the color bar) and instantaneous temperature tendency from the dynamics (TTND, in red contours at intervals of 50 K d^{-1}) after a single timestep at 360 h of integration on the GDPS test grid. Wind

An aside: What do we advect?

Despite the presence of an advective temperature tendency, temperature is not advected in GEM. Instead, each prognostic equation (i) is separated into a total derivative (dF/dt) and forcings (G):

$$\frac{dF_i}{dt} + G_i = 0$$

For arrival points (A, valid at time t) and departure points (D, valid at time t-δt), these terms can be estimated with off-centering b as:

$$\frac{dF_i}{dt} \approx \frac{F_i^A - F_i^D}{\delta t} \qquad G_i \approx bG_i^A + (1-b)G_i^D$$

The time levels can be separated to yield:

$$\frac{F_i^A}{\tau} + G_i^A = \frac{F_i^D}{\tau} - \beta G_i^D \equiv R_i \qquad \text{where} \qquad \tau = b\delta t \qquad \beta = \frac{(1-b)}{b}$$

Since the fields at time level t-δt are known, the advection scheme is thus responsible for advecting the right-hand-side (R) terms of the prognostic equations.

An aside: What do we advect?

The last step of the nonlinear iteration is to recompute the basic state variables through back-substitution. This produces a tendency value for temperature, despite the fact that temperature itself is not an advected quantity.

There are five prognostic right hand sides to advect in hydrostatic GEM4:

$$\vec{R}_h = \frac{\vec{V}_h}{\tau} - \beta\left[f\,\hat{k}\times\vec{V}_h + R\,\bar{T}^{\zeta}\nabla_\zeta(Bs) + \nabla_\zeta\phi' \right]$$ Momentum (u,v)

$$R_T = \frac{1}{\tau}\left[\ln\left(\frac{T}{T_x}\right) - \kappa\, Bs \right] - \beta\left(-\kappa\,\dot{\zeta}\right)$$ Thermodynamic

$$R_c = \frac{1}{\tau}\left[\bar{B}^{\zeta}\, s + \ln\left(1+\delta_\zeta Bs\right) \right] - \beta\left(\nabla_\zeta\cdot\vec{V}_h + \delta_\zeta\dot{\zeta} + \bar{\dot{\zeta}}^{\zeta}\right)$$ Continuity

$$R_\phi = \frac{\bar{\phi'}^{\zeta}}{\tau} - \beta\left(-RT_x\dot{\zeta} - gw\right)$$ Geopotential

The thermodynamic equation is contains a time-derivative of temperature, and is thus most likely to have a direct impact on temperature tendency.

Root Cause Analysis of Error

Thermodynamic RHS and Dynamics Temperature Tendency

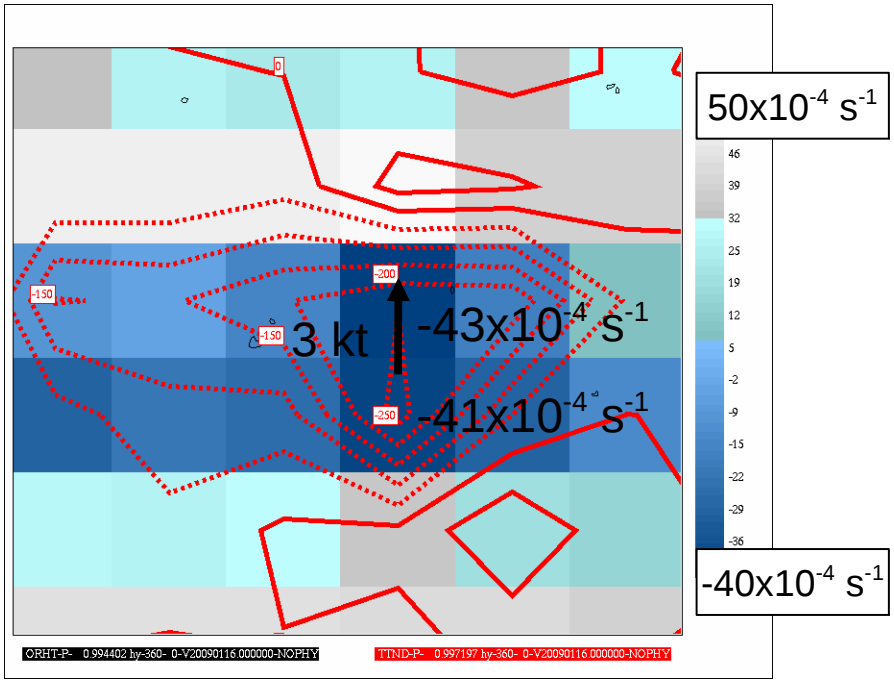

Lowest-level R_T (shaded in x10^{-4} s^{-1} as indicated on the color bar) and instantaneous temperature tendency from the dynamics (TTND, in red contours at intervals of 50 K d^{-1}) after 360 h of integration on the GDPS test grid.

Temperature

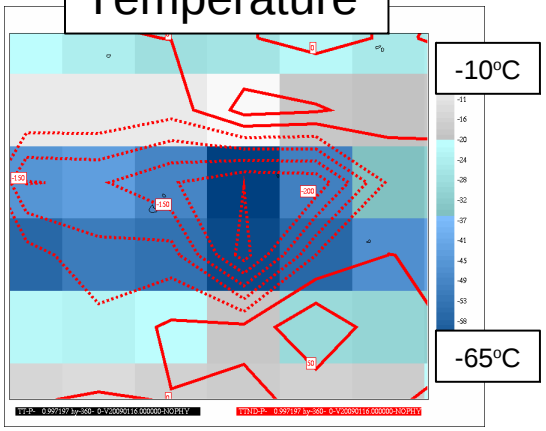

As for the panel on the left, but with temperature shaded.

The structure of the advected R_T field (left) looks very similar to that of the temperature field (above) because of the form of the thermodynamic equation.

The sharp gradients in the RT field will be problematic for the cubic interpolation of the advection scheme.

Root Cause Analysis of Error

Thermodynamic RHS and Dynamics Temperature Tendency

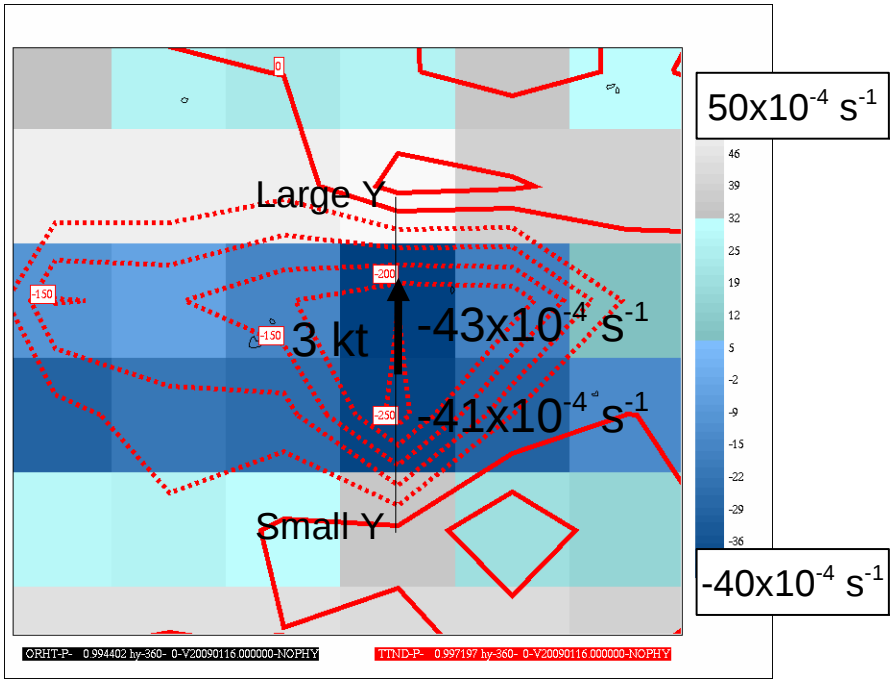

Lowest-level R_T (shaded in x10^{-4} s^{-1} as indicated on the color bar) and instantaneous temperature tendency from the dynamics (TTND, in red contours at intervals of 50 K d^{-1}) after 360 h of integration on the GDPS test grid.

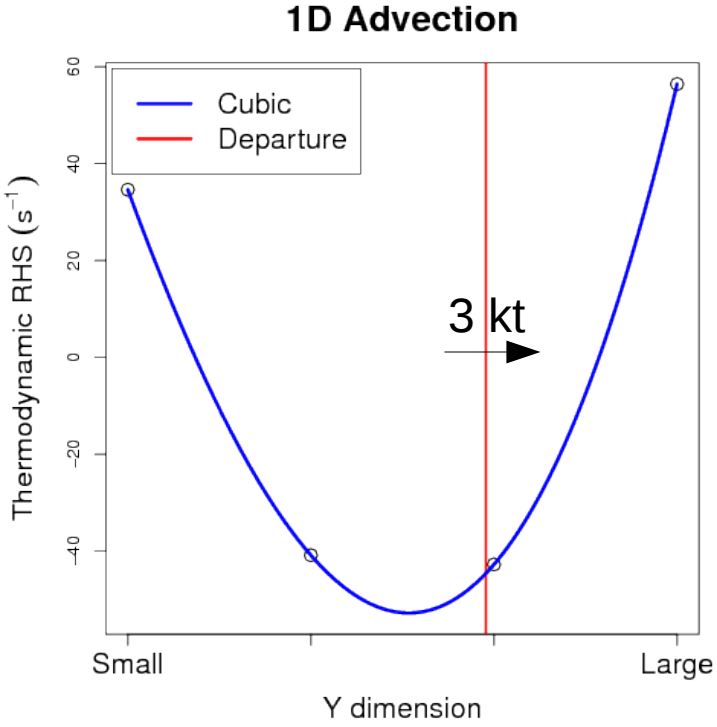

Section of R_T as shown to the left.

The undershoot of the cubic interpolation leads to negative advection of R_T, and thus a negative temperature tendency following back-substitution.

Root Cause Analysis of Error

Thermodynamic RHS and Dynamics Temperature Tendency

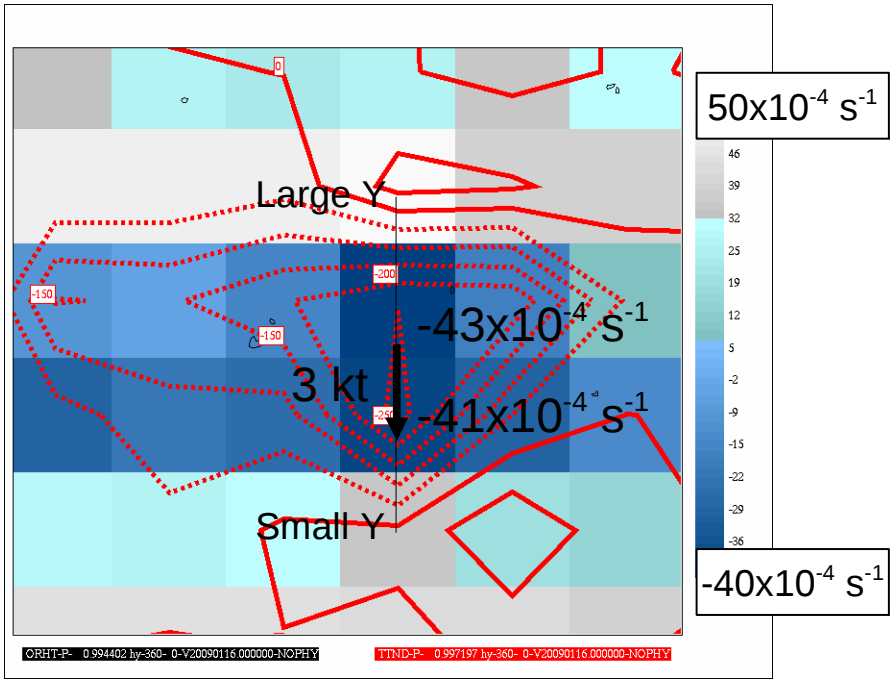

Lowest-level R_T (shaded in x10^{-4} s^{-1} as indicated on the color bar) and instantaneous temperature tendency from the dynamics (TTND, in red contours at intervals of 50 K d^{-1}) after 360 h of integration on the GDPS test grid.

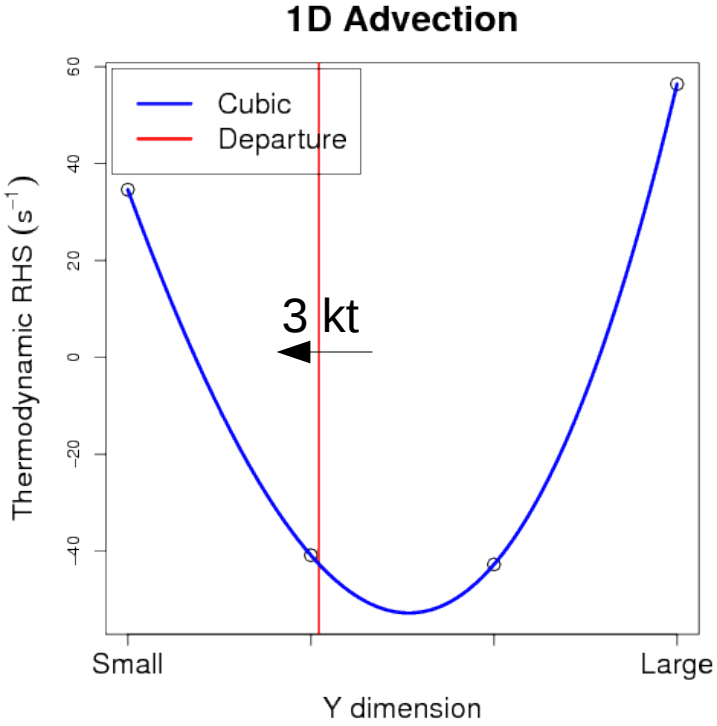

Section of R_T as shown to the left.

A similar interpolation undershoot occurs at the neighbouring point.

The combined effect of these undershoots is to simultaneously cool the two VCP points.

Root Cause Analysis of Error

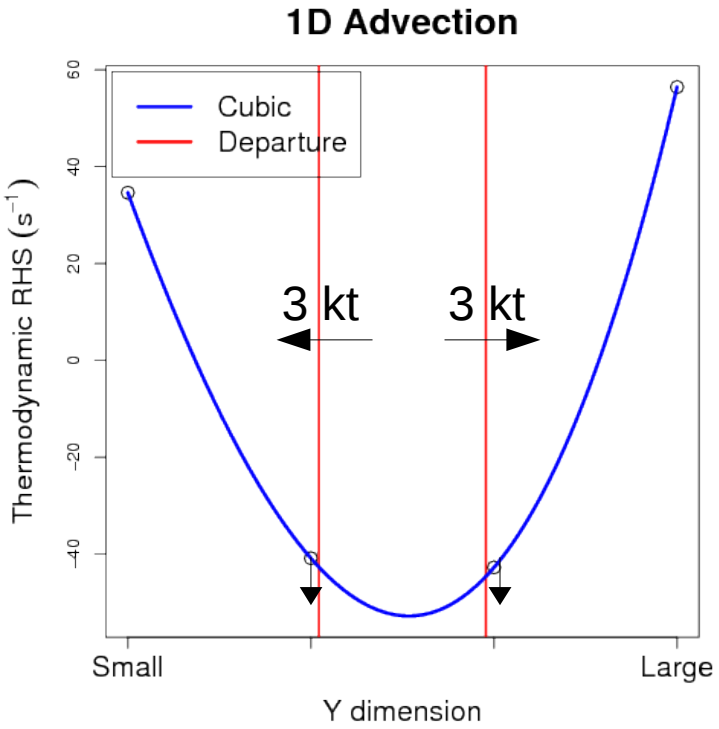

Section of R_T advection in the VCP.

Over/undershoots in cubic interpolation are features that limit the diffusive nature of the semi-Lagrangian advection scheme: they are not errors in themselves.

The structure of the basin orography is extremely important: a valley floor width of two gridpoints means that the fitted cubic function will have the maximum overshoot in the middle of the VCP.

Diverging flow from the centre of the VCP is consistent with the decoupling of the stable cold air and provides ideal conditions for the “digging out” of the low RT values in the VCP by advection.

Root Cause Analysis of Error

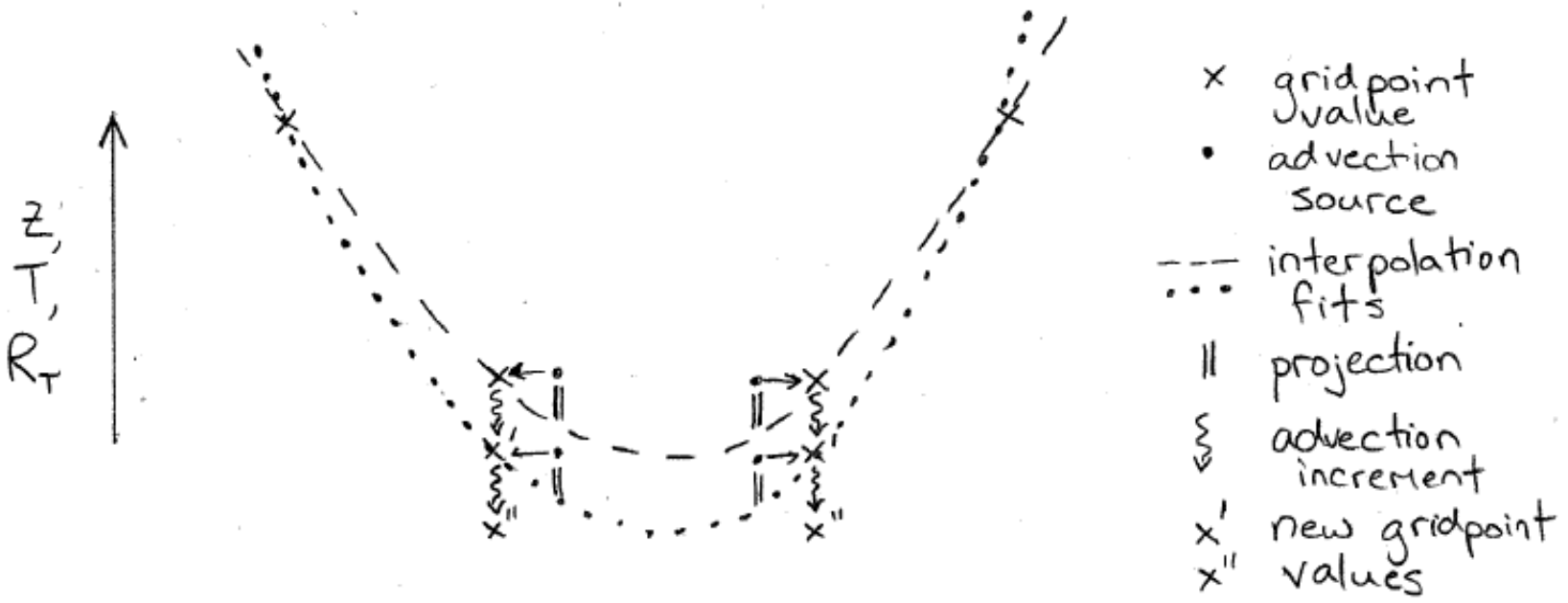

Schematic showing VCP over-cooling for an imposed diffluent 1D wind field from the perspective of the advection scheme for two time-steps.

- As gradients between the basin floor and the surrounding high terrain increase, so does the extent of the undershoot in the VCP
- The cold pool is stationary since it is anchored to orography: as long as synoptic forcing and warming from physical processes remain weak, the numerical “digging” will continue to cool the basin

Validation of Cooling Mechanism

- Use of the limited (50x50 gridpoint) step-driven LAM domain means that the local environment is relatively unaffected by model modifications (integration does not diverge)
- With interpolation under/overshoots prevented during the advection of R_T, no VCP over-cooling occurs

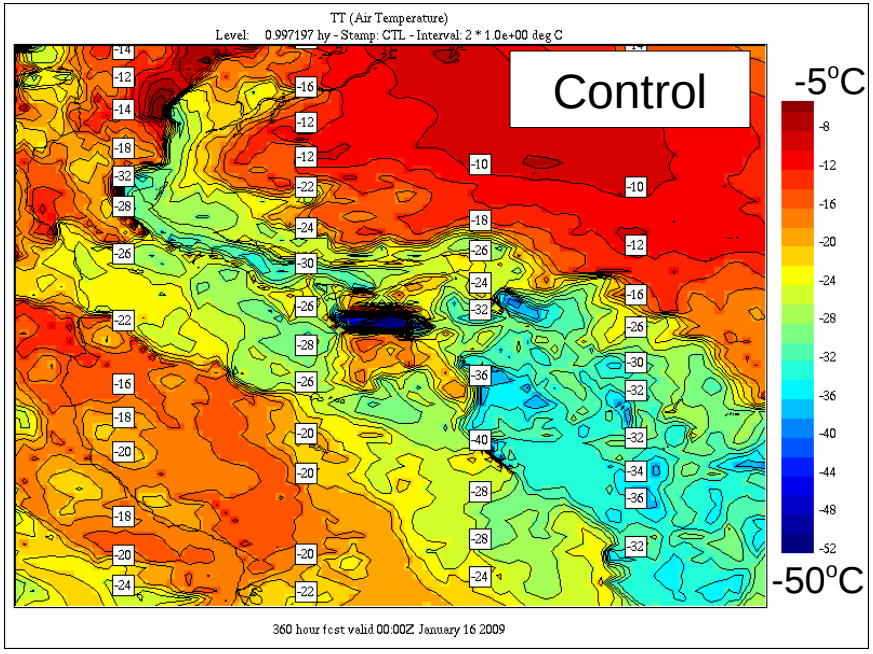

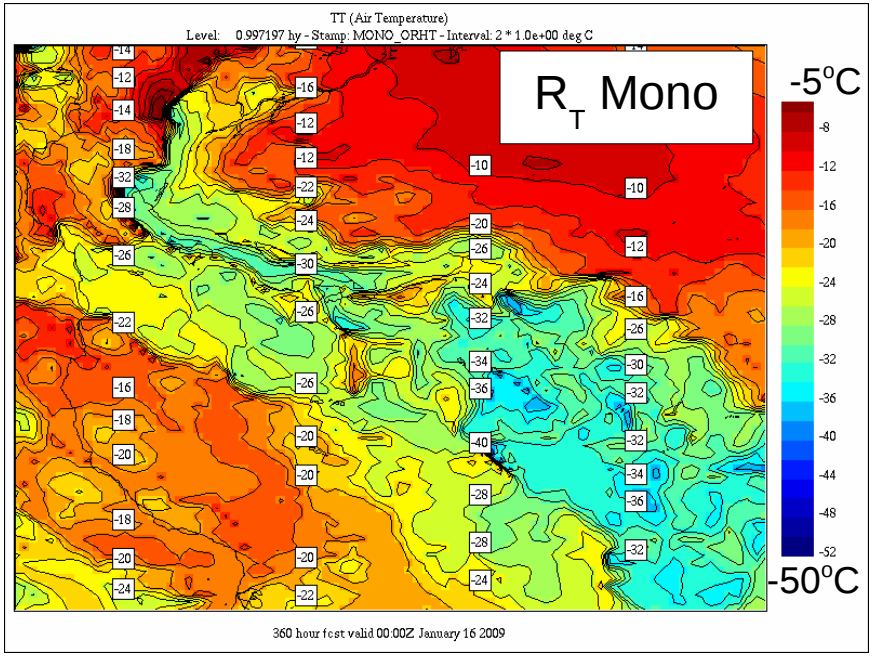

Lowest-level temperature after 15 days in the control (left) and monotonic R_T (right) limited-area integrations stepwise-driven from the "perpetual winter" YEC-15 simulation.

Validation of Cooling Mechanism

The fact that under/overshoot elimination in R_T advection eliminates VCP over-cooling suggests strongly that the proposed numerical cooling mechanism is responsible for this event.

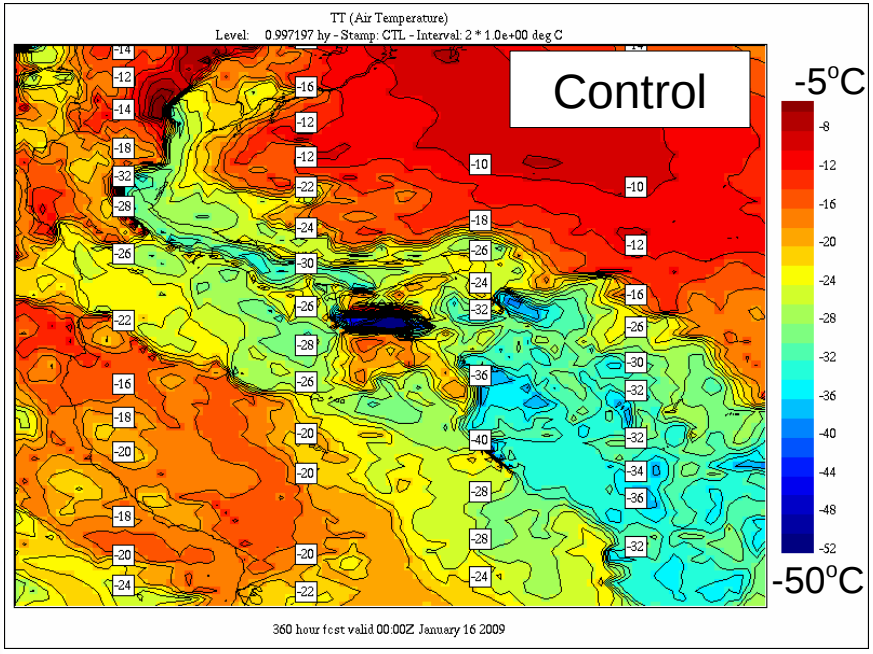

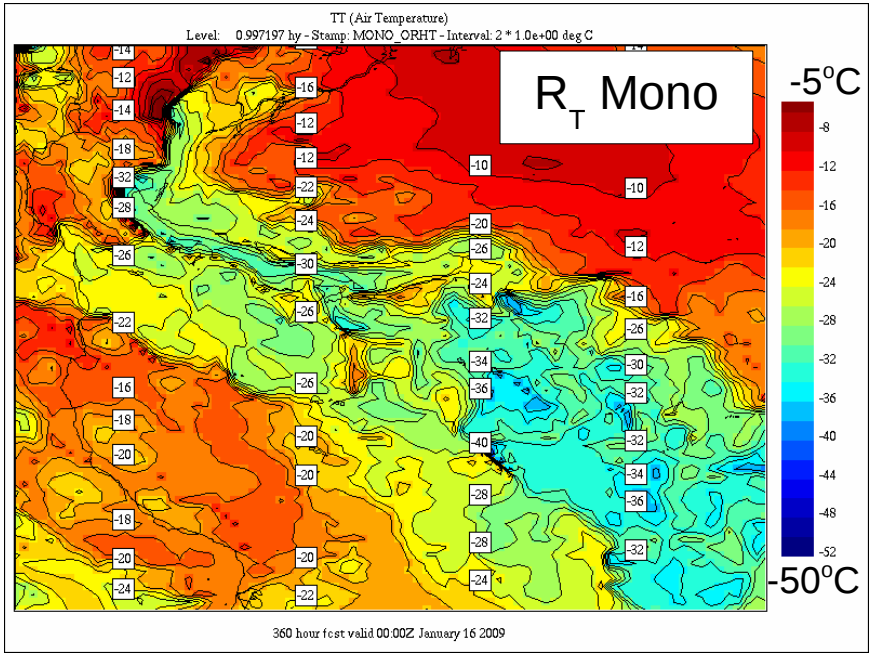

Lowest-level temperature after 15 days in the control (left) and monotonic R_T (right) limited-area integrations stepwise-driven from the "perpetual winter" YEC-15 simulation.

Ingredients of a VCP Cooling Event

- The model pathology is a result of numerically-induced cooling that occurs under very specific conditions:
  - Persistently weak synoptic-scale flow (does not displace VCP)
  - Presence of a basin in the orographic field (VCP trapped)
  - Matching of basin scale to model grid spacing (two gridpoints on the basin floor to maximize undershoot after curve-fitting)
  - Alignment of the basin secondary axis with the grid
  - An initial cooling mechanism (begins establishing thermal gradients)
  - Weak diffluent flow in the VCP (sustains overshoots)
- Once VCP over-cooling has started, only a physical process or change in the synoptic-scale flow appears to be capable of limiting the cooling feedback
- The rate of numerical cooling appears to be highly resolution-dependent, which may explain the recent emergence of the problem (2.5 km HRDPS, 15 km YEC)

Development of Diffluent Flow

So far, the diffluent near-surface flow has been either diagnosed or imposed; however, it is critically important for the maintenance of the numerical cooling

Where does the diffluent flow come from, and how is it maintained?

1) Cooling begins at lower levels through physical process (e.g. nocturnal clear-sky radiation)
2) Thickness is reduced relative to the undisturbed column
3) Upper and lower isobars are displaced downwards and upwards
4) Isallohypsic wind is divergent at lower levels and convergent above
5) Surface pressure increase implies a net convergence in the VCP column

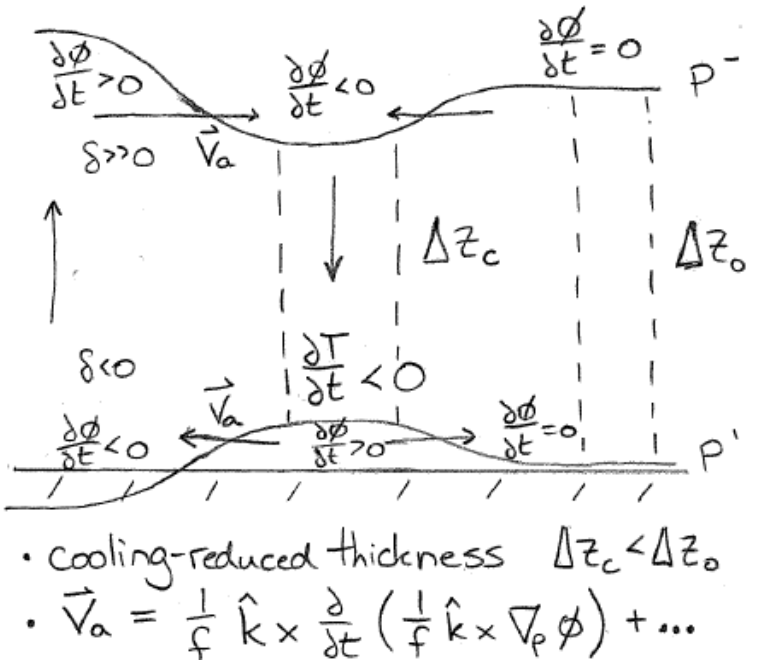

Schematic of hydrostatic response to cooling in the column.

Development of Diffluent Flow

So far, the diffluent near-surface flow has been either diagnosed or imposed; however, it is critically important for the maintenance of the numerical cooling

Where does the diffluent flow come from, and how is it maintained?

6) Flanking columns experience net divergence concentrated at upper levels
7) A thermally-direct secondary circulation develops to balance numerical cooling
8) The divergent lower-level winds lead to numerical undershoot-induced diabatic cooling
9) The cooling further reduces column thickness and reinforces the VCP feedback at step 2

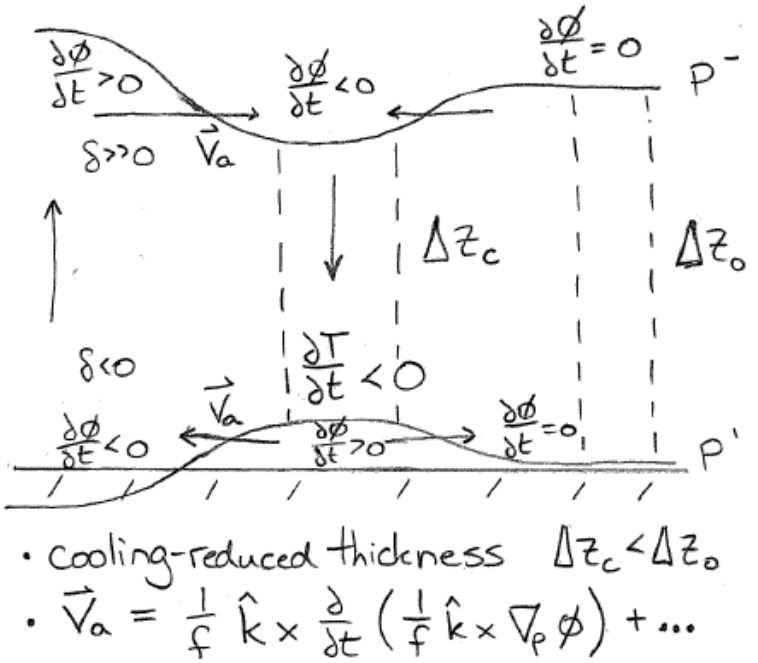

Schematic of hydrostatic response to cooling in the column.

Development of Diffluent Flow

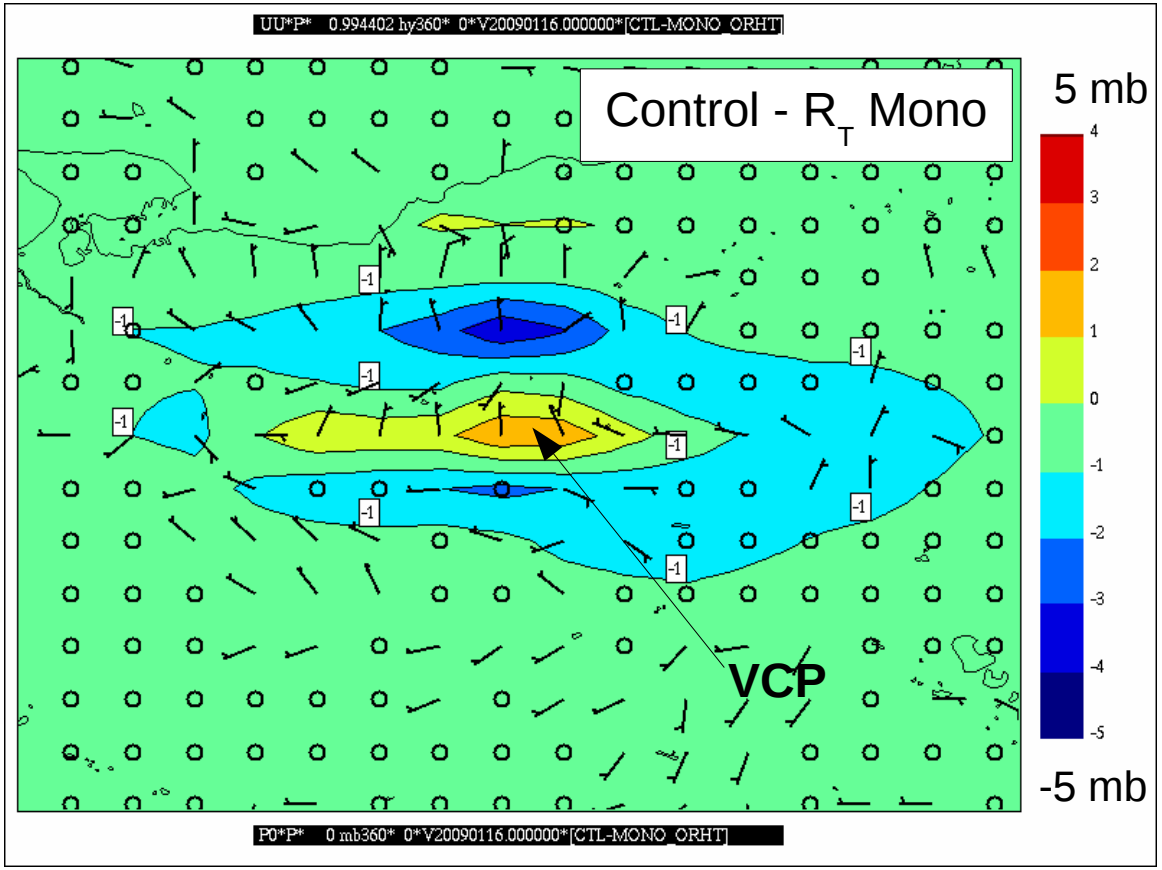

Differences (Control – R_T Mono) representing surface pressure (shaded) and wind (black barbs) patterns associated with the VCP over-cooling event that occurs after 15 days of integration in the "perpetual winter" YEC-15 configuration.

High pressure develops in the cold basin, along with divergent near-surface winds.

Flanking low created by net convergence into the VCP column, possibly enhanced by gravity waves.

Both the surface pressure and wind patterns associated with VCP over-cooling are consistent with the presented conceptual model.

Severe Storm Mesohigh Analog

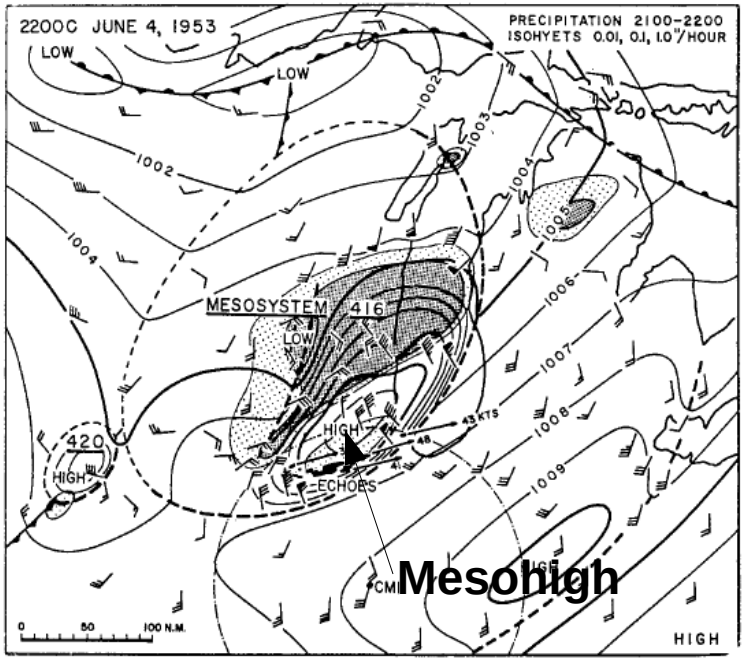

Mesoanalysis of the 2200 CST 4 June 1953 squall line in Illinois. Pressure (contours), winds (barbs), precipitation (stippled) and radar reflectivity (dark shaded) are shown simultaneously (Fujita and Brown 1958).

Mesohigh formation is well-documented in severe storms literature: highs form primarily as a result of evaporative cooling in precipitation downdrafts.

Cooling mechanisms are different, but the response pressure and wind response is similar to VCP over-cooling; however precipitation-induced mesohighs are not fixed to topography.

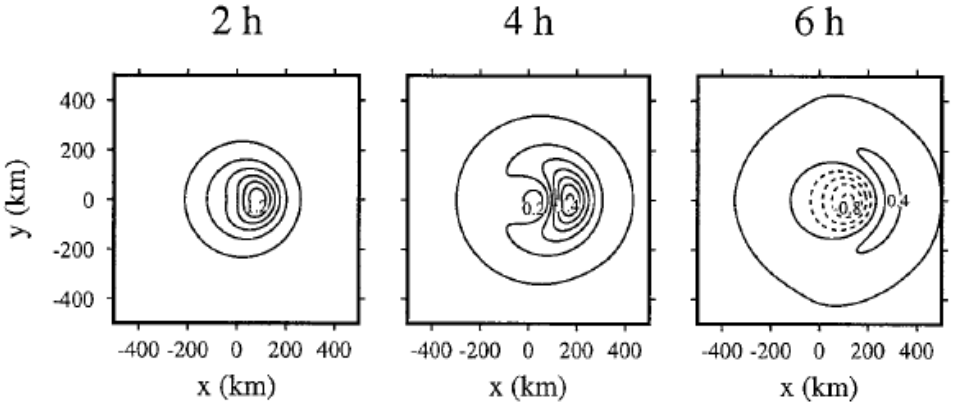

Pressure response to a moving axisymmetric cooling in a linearized dynamical system (contour interval 0.2 mb; Haertel and Johnson 2000).

Evolution of a VCP Cooling Event

1) Physical process (e.g. overnight radiative cooling) create a realistic VCP in a small basin, with a weak internal flow separated from the ridge-level winds
2) The localized cooling creates a weak meso-high with an initially-small diffluent flow
3) The scale and orientation of the basin lead to small, sustained undershoots in the advection scheme
4) Each undershoot results in diabatic cooling, and the reinforcement of the meso-high and divergent flow in the VCP
5) The feedback of numerical cooling ensures that the temperature perturbation increases as steps 2-5 repeat
6) The VCP over-cooling event ends only if the cold air is dug out by enhanced synoptic-scale winds or if a physical process (e.g. solar insolation) is able to halt the cooling cycle

Possible VCP Over-Cooling in R2?

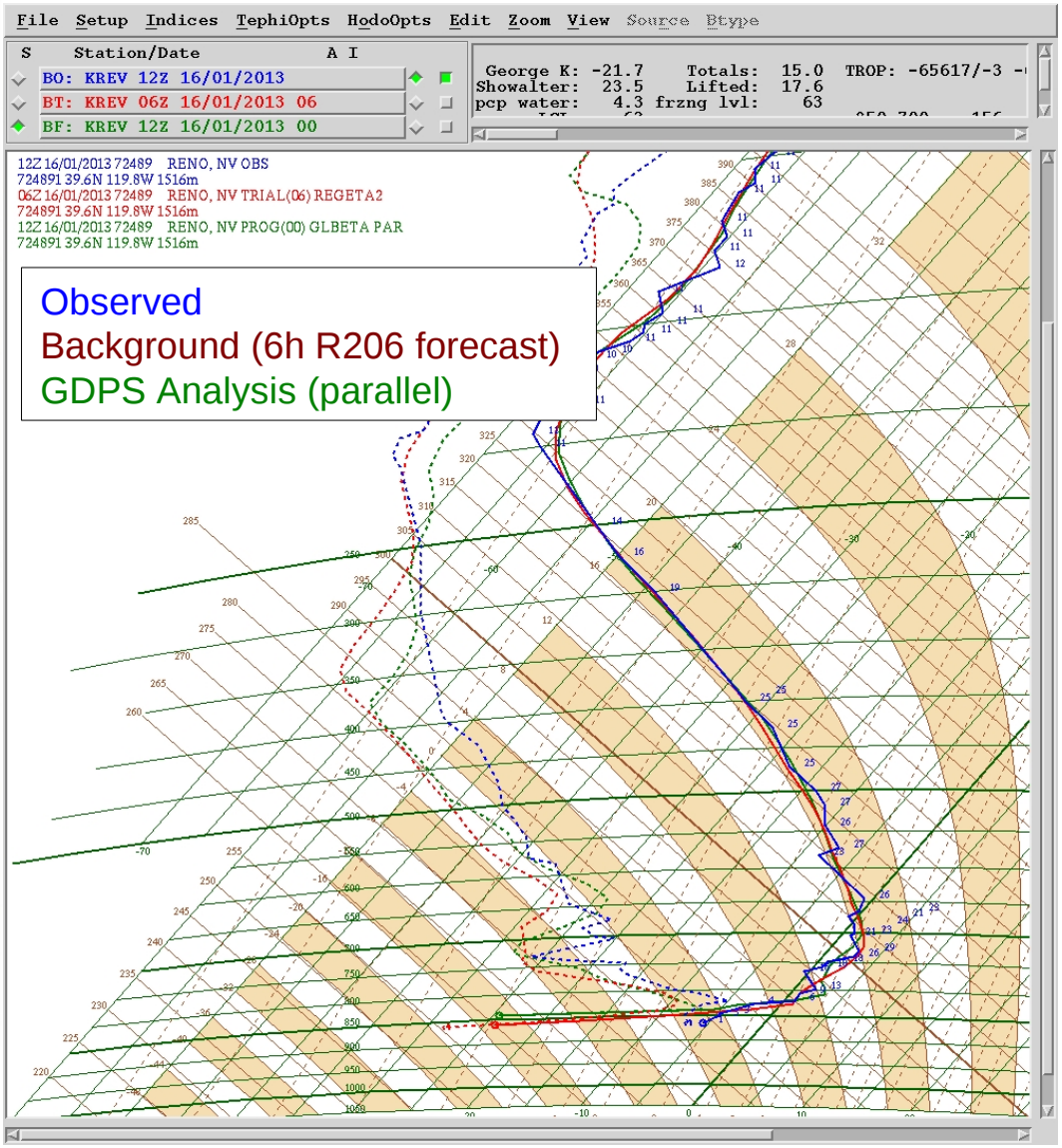

A&P (Diane Ouellet) noted a Reno, NV radiosonde rejection in the 1200 UTC 16 January R2 assimilation cycle resulted from a shallow cold departure in the background.

Since a profile is insufficient to determine whether a cold error is the result of VCP over-cooling, further investigation was required.

Balloon (blue) and model (red and green) soundings for Reno, NV (RNO), taken at 1200 UTC 16 January 2013 (D. Ouellet)

Possible VCP Over-Cooling in R2?

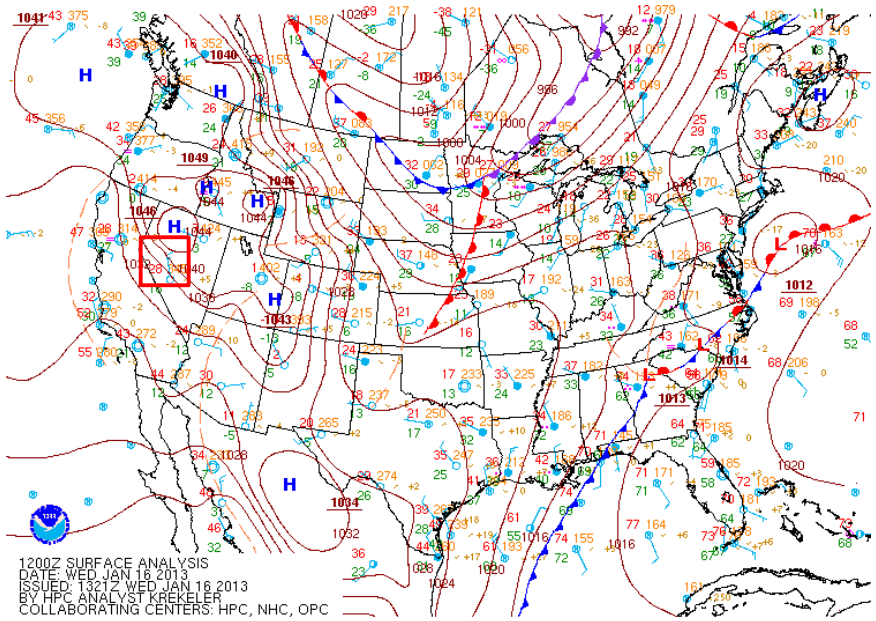

Surface analysis for 1200 UTC 16 January 2013 from HPC.

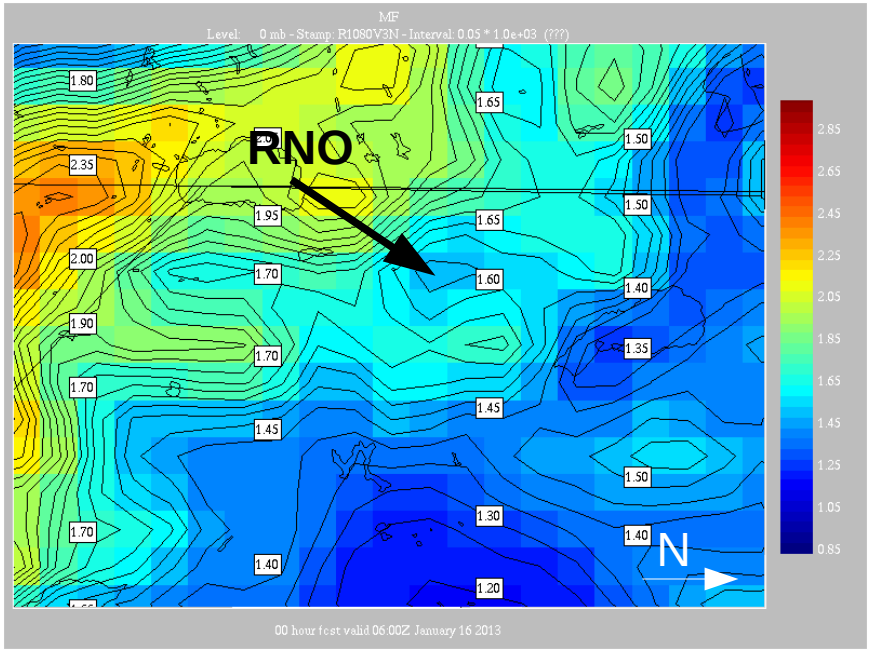

Model orography field from the R2 trial GEM configuration (RNO indicated, note 90^{o} rotation)

Synoptic scale forcing is relatively weak, with winds in the RNO metar light and variable: possibly supportive of VCP over-cooling.

The RNO gridpoint is located in a basin, with a width of two gridpoints in the model Y-direction: possible over-cooling configuration, but quite shallow

Possible VCP Over-Cooling in R2?

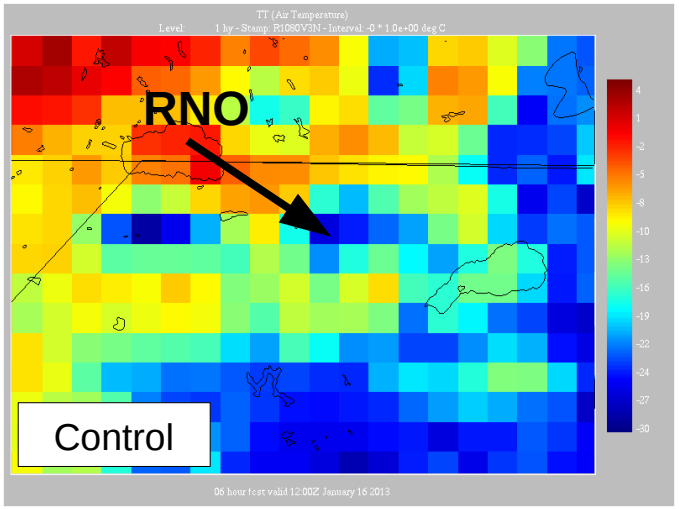

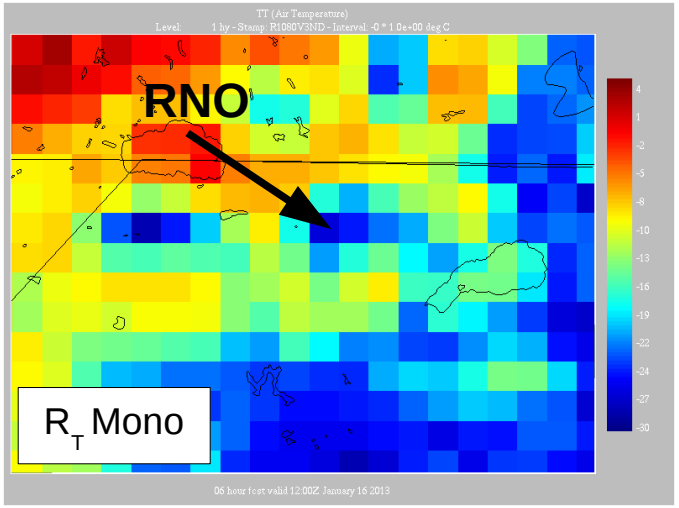

Near-Surface Temperature

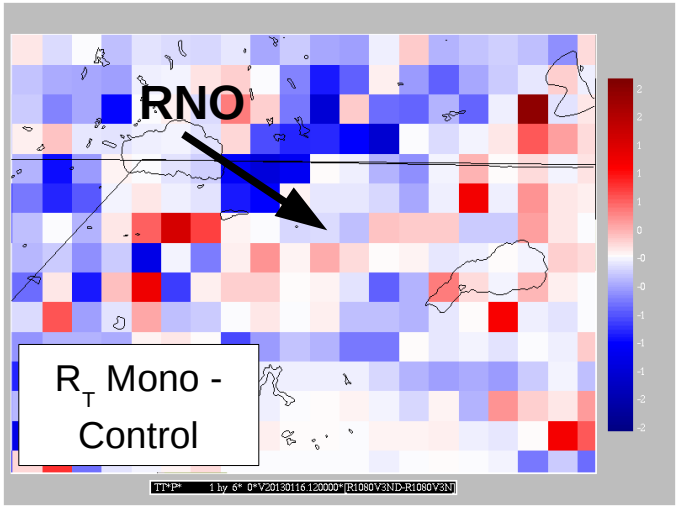

A rerun using monotonic advection for R_T does not impact temperatures in the Reno basin.

Background (6 h fcst) near-surface temperatures in the R206 trial (top) and a rerun with over/undershoots eliminated for R^T advection (bottom) for the 0600 UTC 16 January 2013 integration. Difference is shown above.

Possible VCP Over-Cooling in R2?

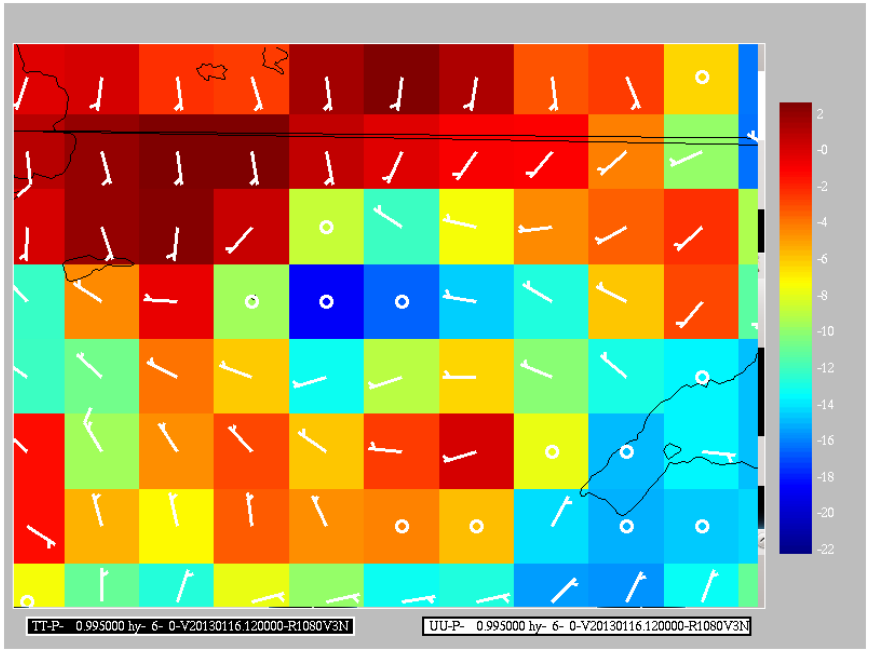

Background (6 h fcst) near-surface temperatures in the R206 trial (shaded) and winds (white barbs) for the 0600 UTC 16 January 2013 integration, valid 1200 UTC 16 January.

Despite the moderately-favourable topographic configuration, and strong lower-level inversion in the basin, the VCP over-cooling feedback does not occur because diffluent winds do not appear in the stagnant cold pool.

In this case, the source of the cold forecast error does not appear to be related to numerical cooling: other physical error sources exist that may explain the 10-15 K error.

Not all cold errors in complex terrain are related to VCP over-cooling: they will not necessarily be fixed by the solutions discussed here

A VCP Cooling Solution: θ-Diffusion

- The nature of the pathological behaviour involved in VCP over-cooling is now well understood
- One possible solution will be to limit GEM's ability to create the shocks (gradients) that are a key element of the feedback process
- In addition to the current horizontal diffusion on the three wind components, an option to diffuse potential temperature has been introduced in GEM 4.4.3
- The diffusion of a conserved field is required to avoid artificial sources/sinks of heat along sloped model surfaces
- The inclusion of θ-diffusion fixes all known over-cooling events
- The effect of θ-diffusion on the model configurations that suffered from VCP over-cooling is minor except in HRDPS
- Other possible solutions will be discussed at the end

θ-Diffusion in the HRDPS

- All operational HRDPS windows currently run with (relatively) strong ∇^4, 0.4 diffusion on u, v and zeta-dot
- The diffusion coefficient was doubled (from 0.2) following a West window VCP over-cooling event
- The increased coefficient was found to reduce over-cooling in that event; however, it has since been unable to prevent West, Arctic and National grid failures
- The introduction of θ-diffusion eliminates VCP over-cooling in all known HRDPS cases
- Numerical diffusion can be reduced to ∇^6, 0.04 consistent with other systems and the unphysical nature of this process

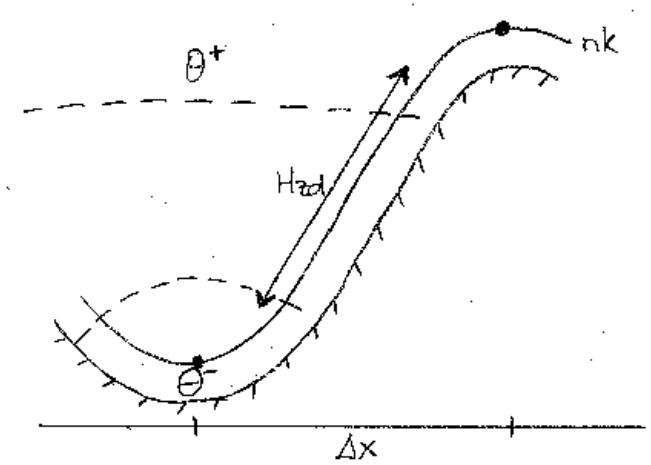

Schematic of diffusion for small ∇θ: weak mixing in weak static stability.

θ-Diffusion in the HRDPS

- All operational HRDPS windows currently run with (relatively) strong ∇^4, 0.4 diffusion on u, v and zeta-dot
- The diffusion coefficient was doubled (from 0.2) following a West window VCP over-cooling event
- The increased coefficient was found to reduce over-cooling in that event; however, it has since been unable to prevent West, Arctic and National grid failures
- The introduction of θ-diffusion eliminates VCP over-cooling in all known HRDPS cases
- Numerical diffusion can be reduced to ∇^6, 0.04 consistent with other systems and the unphysical nature of this process

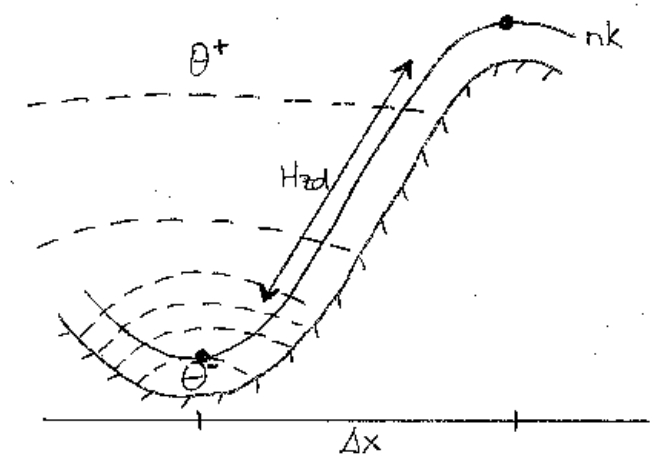

Schematic of diffusion for large ∇θ: strong mixing despite strong static stability.

θ-Diffusion in the HRDPS (National)

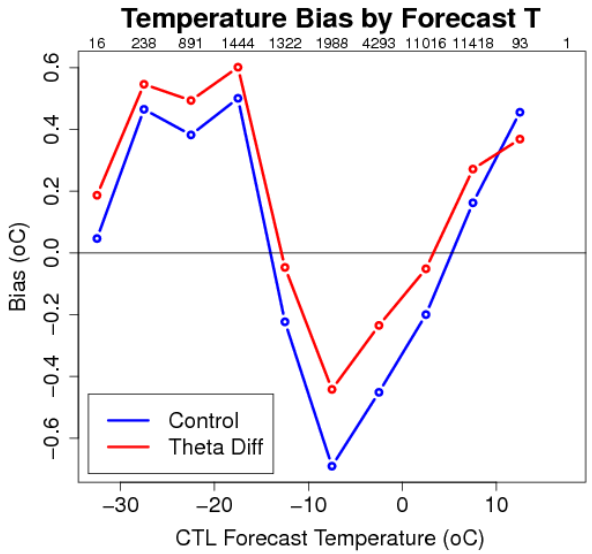

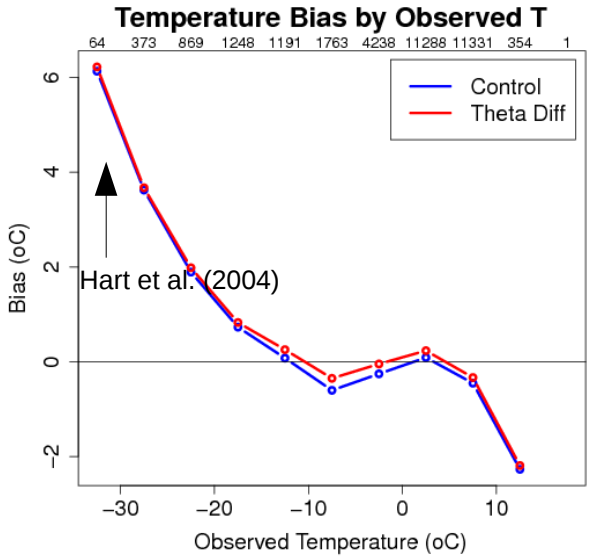

The dominant impact of θ-diffusion on the HRDPS is in the near-surface air temperature.

Warming occurs across a range of predicted temperatures, consistent with most observations being in valleys: diffusion along model surfaces mixes high potential temperature air down from the peaks.

Strong warm bias for cold observed temperatures suggests mixing-out of inversions, consistent with a limited impact of θ-diffusion since gradients are eliminated by the PBL scheme (hypothesis).

Near-surface temperature bias in 40 winter cases on the National grid, computed over British Columbia with all lead times combined. The number of events in each bin is identified at the top of the plot.

θ-Diffusion in the HRDPS (National)

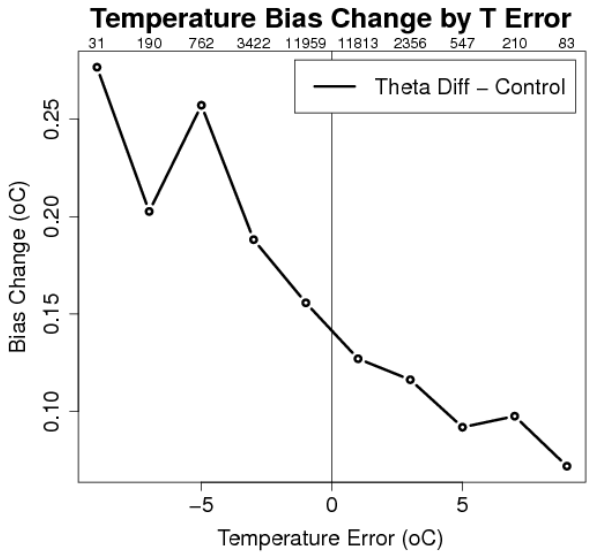

Near-surface temperature bias change between the Control and θ-diffusion experiment in 40 winter cases on the National grid, computed over British Columbia with all lead times combined (θ-Diffusion – Control, such that positive values denote warming). The number of events in each bin is identified at the top of the plot.

Environments representative of cold errors (negative values on the x-axis) are warmed more than environments associated with warm errors: the negative slope implied an overall bias reduction.

Numerical gradient-induced cooling may have had an impact on guidance, since its reduction by diffusion acts primarily under cold error conditions, consistent with the reduction of VCP over-cooling.

Cold errors therefore appear to be associated with strong gradients, consistent with the VCP over-cooling process occurring in non-bowl topographies where the generated cold air flows away from the source region.

θ-Diffusion in the HRDPS (West)

Unlike the HRDPS National configuration, the West window has a warm bias in its current implementation: θ-diffusion valley warming is thus negative in the surface scores on this domain.

The current θ-diffusion implementation will therefore be proposed as a backup plan in the case of a VCP over-cooling-induced model failure in the current HRDPS system.

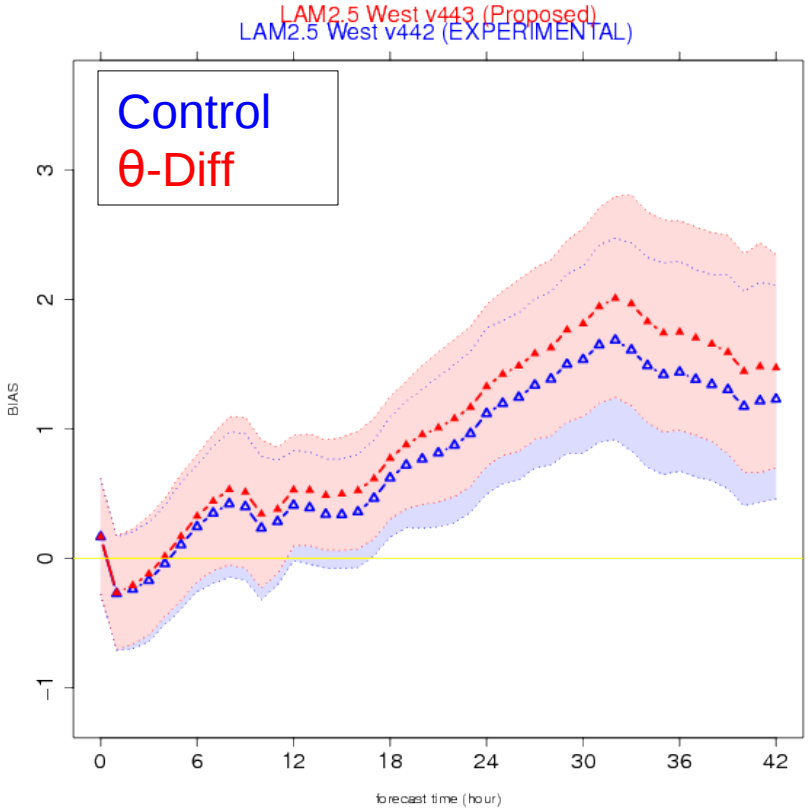

Near-surface temperature bias by forecast hour in the operational West window configuration for the control (blue) and θ-diffusion experiment (red). Score is computed at stations whose elevation is within 100 m of that of the corresponding model grid point.

θ-Diffusion in the HRDPS (West)

In a selected case, it appears that valley warming is not offset by cooling at the peaks, leading to an unexpected overall increase in near-surface temperature.

This warming is essentially absent when tests are performed without physics, suggesting that one or more parameterizations may be responding to θ-diffusion.

This behaviour has not been observed in the other GEM configurations: more study of the unexpected response in the HRDPS context is required.

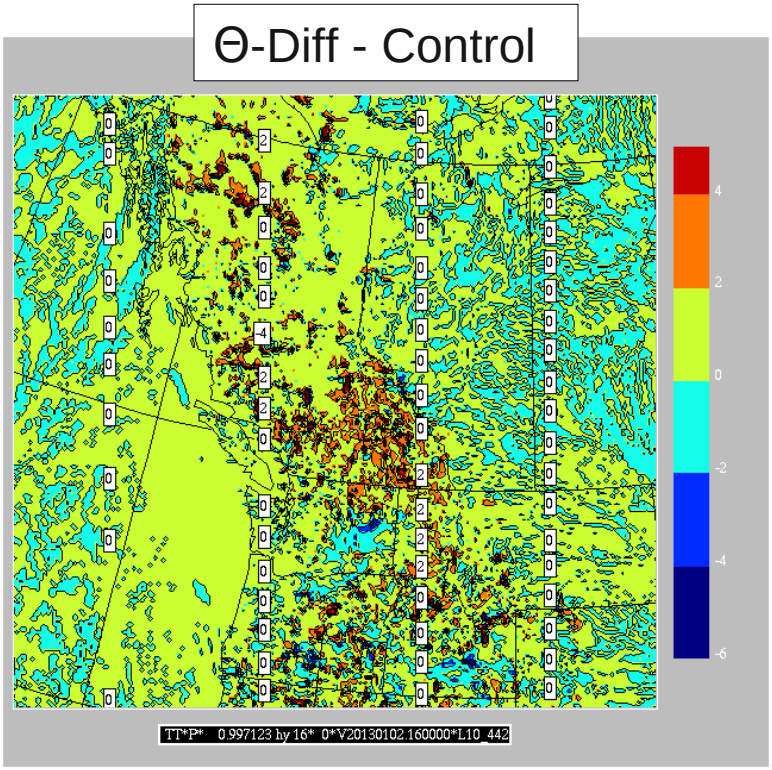

Difference (θ-diffusion – Control) in near-surface temperature guidance in the 16 h forecast of the low resolution (10 km) driver of the HRDPS system for a run initialized at 0000 UTC 2 January 2013.

θ-Diffusion in YEC-15 Forecasts

Diffusion of θ has no impact on upper-air scores in the YEC-15 configuration.

This is a positive result since the mode of model failure is suppressed while the results are left unaffected.

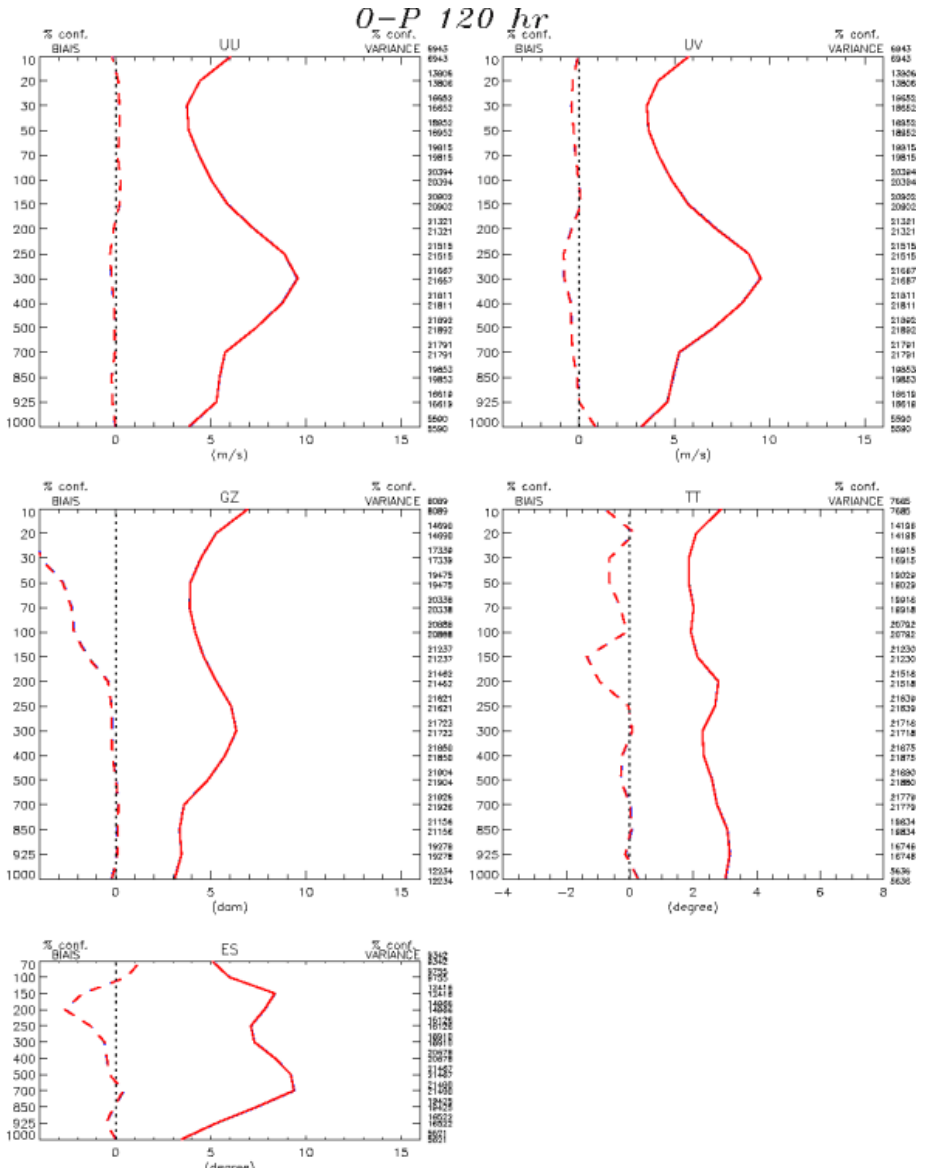

Global Arcad scores for the 120 h forecast of 44 Northern Hemisphere winter cases from the Control (blue) and -diffused (red) GDPS using the YEC-15 configuration.

θ-Diffusion in YEC-15 Climate

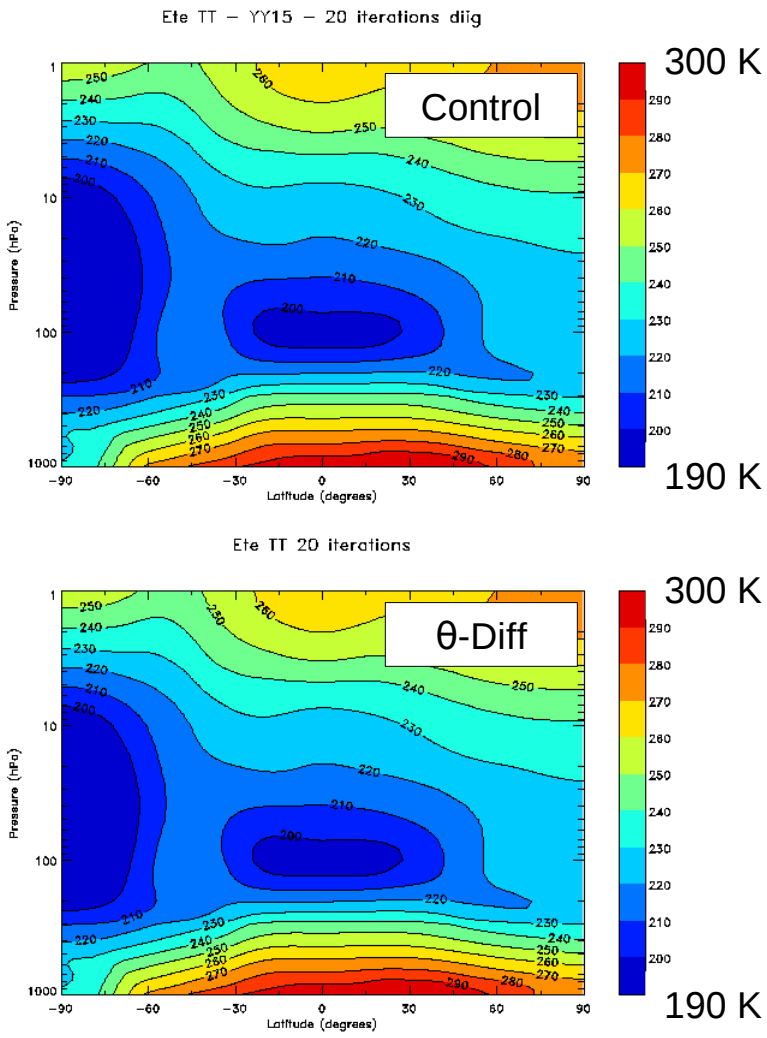

Zonal-Mean Temperatures

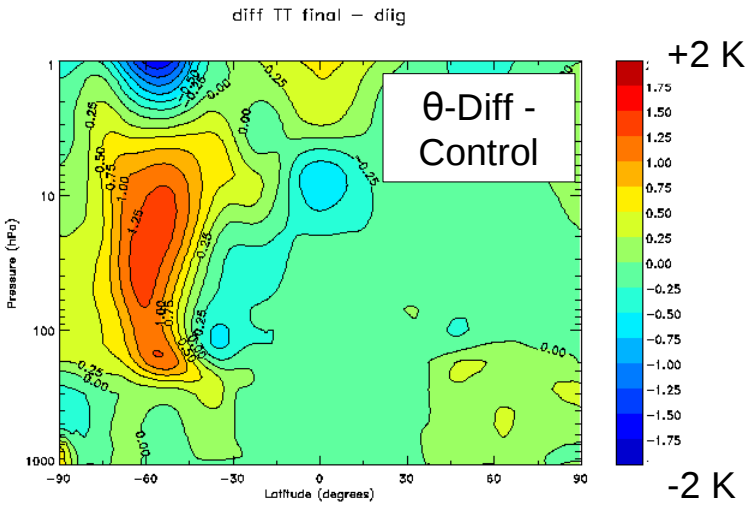

Diffusion of θ weakens the baroclinic zone in the winter midlatitudes, but the effect is imperceptible in the mean fields.

Zonal-mean temperatures in a 20-iteration YEC-15 perpetual July integration (M. Roch).

θ-Diffusion in YEC-15 Climate

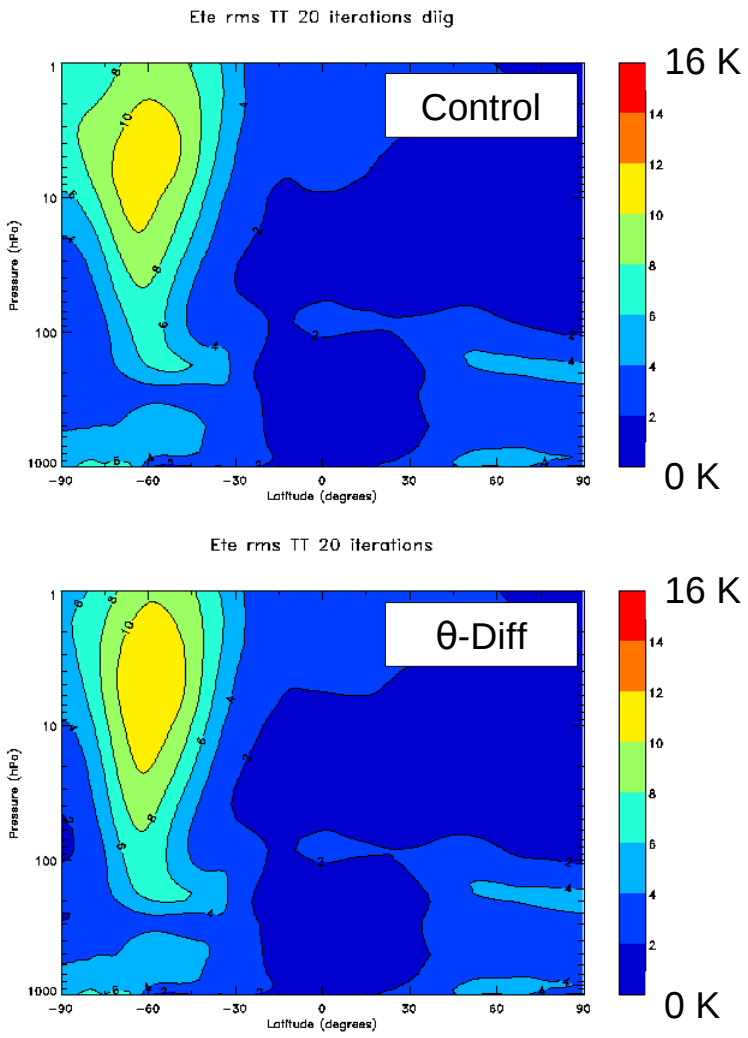

Zonal-Mean T Variability

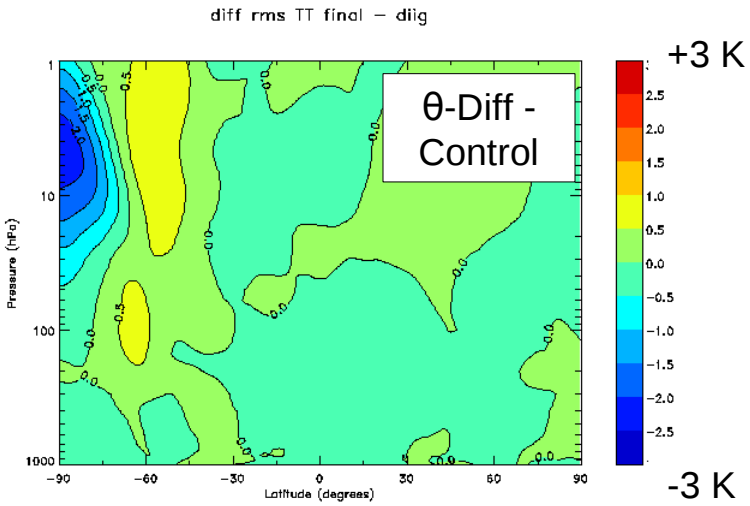

Diffusion of θ limits temperature variance primarily near the pole, where diffusion acts much more strongly.

Zonal-mean temperature std dev in a 20-iteration YEC-15 perpetual July integration (M. Roch).

θ-Diffusion in YEC-15 Climate

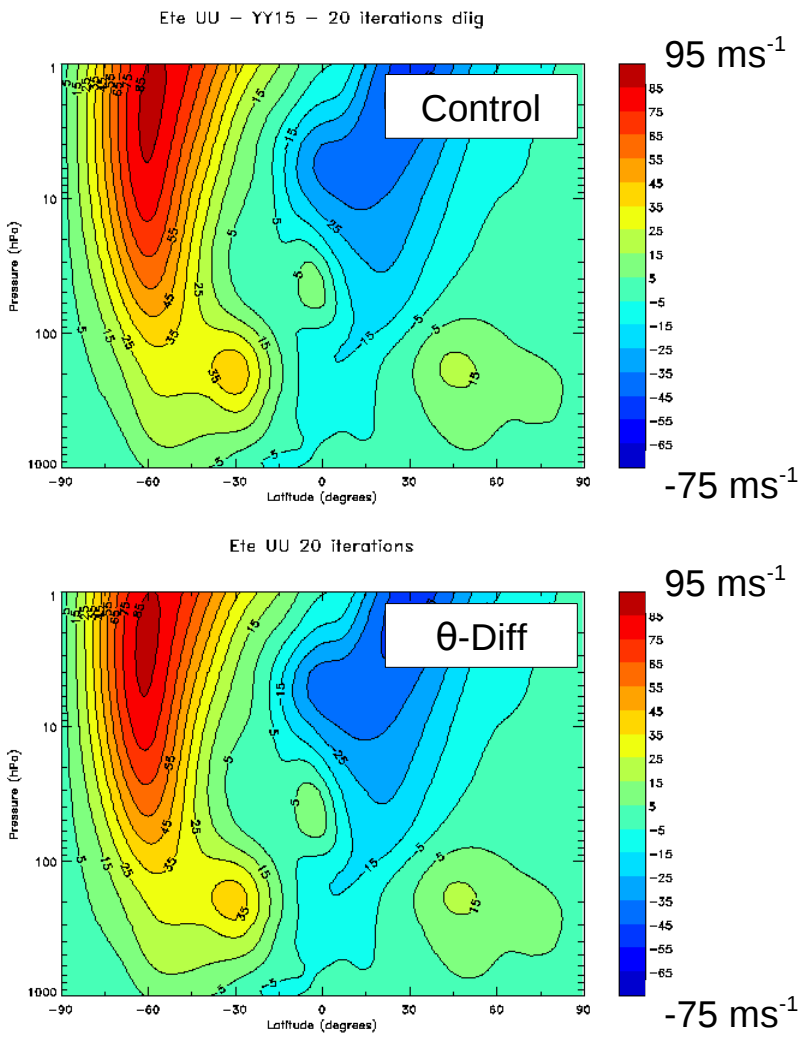

Zonal-Mean Zonal Winds

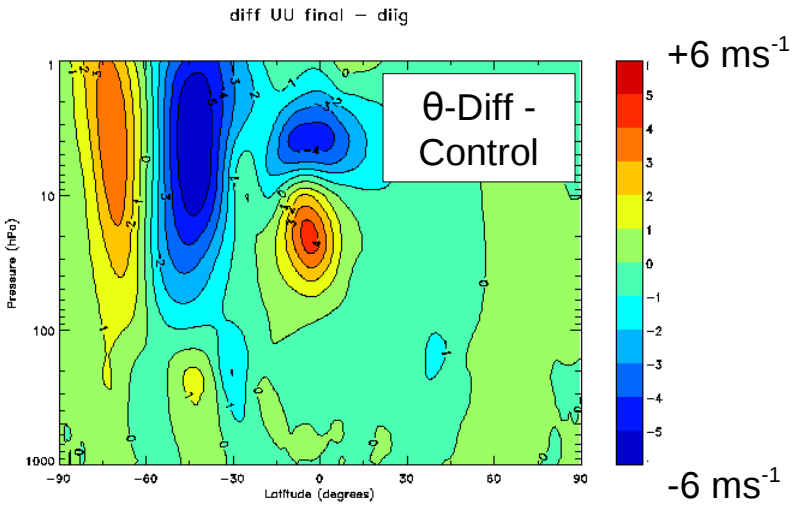

Stratospheric jet is slightly weakened and displaced northward.

Source of equatorial differences is unknown.

Zonal-mean zonal winds in a 20-iteration YEC-15 perpetual July integration (M. Roch).

θ-Diffusion in YEC-15 Climate

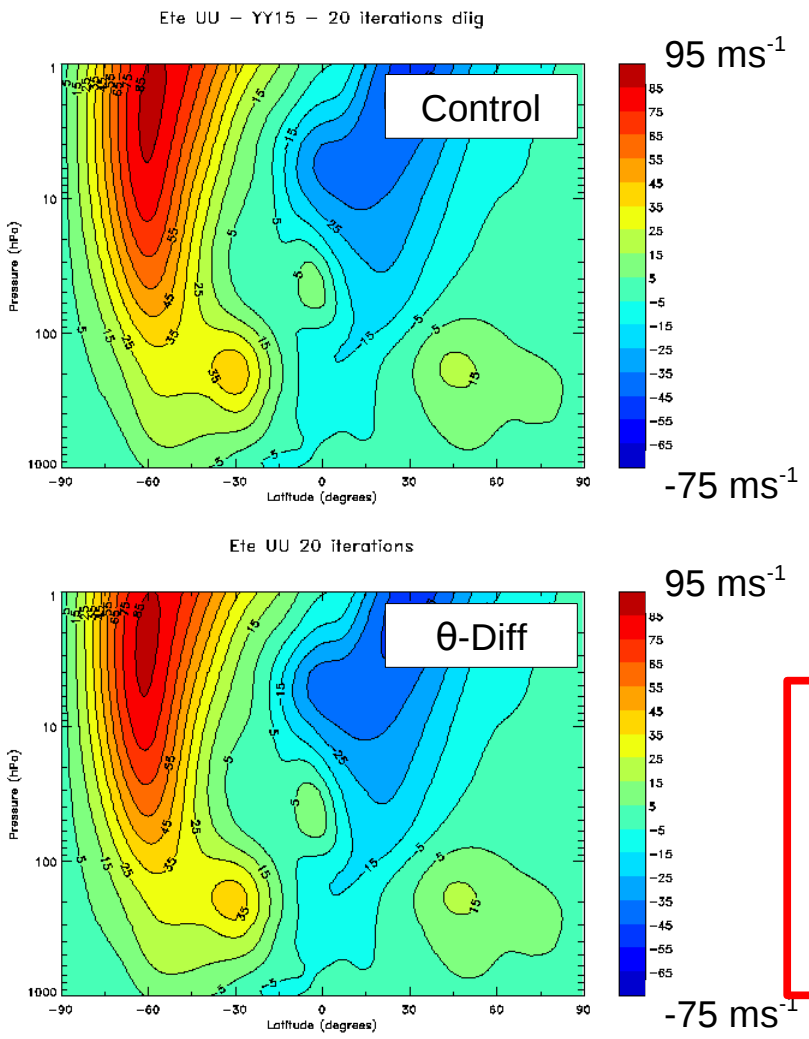

Zonal-Mean Zonal Winds

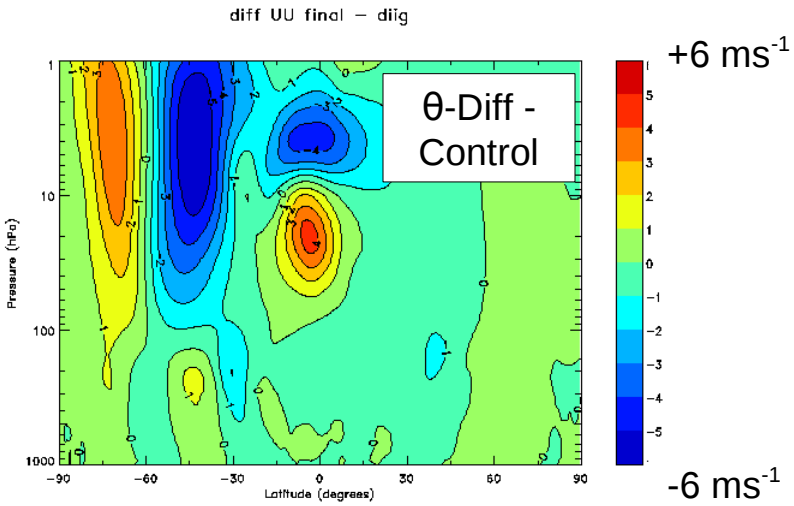

The changes to GEM climate are small and can generally be understood through gradient reduction and resulting changes in the thermal wind.

Zonal-mean zonal winds in a 20-iteration YEC-15 perpetual July integration (M. Roch).

θ-Diffusion and Conservation

- Because we are diffusing a conserved variable, we would not expect θ-diffusion to cause problems
- If systematic overshoots were common in the free atmosphere, then some improvement in conservation might result from θ gradient reduction from diffusion

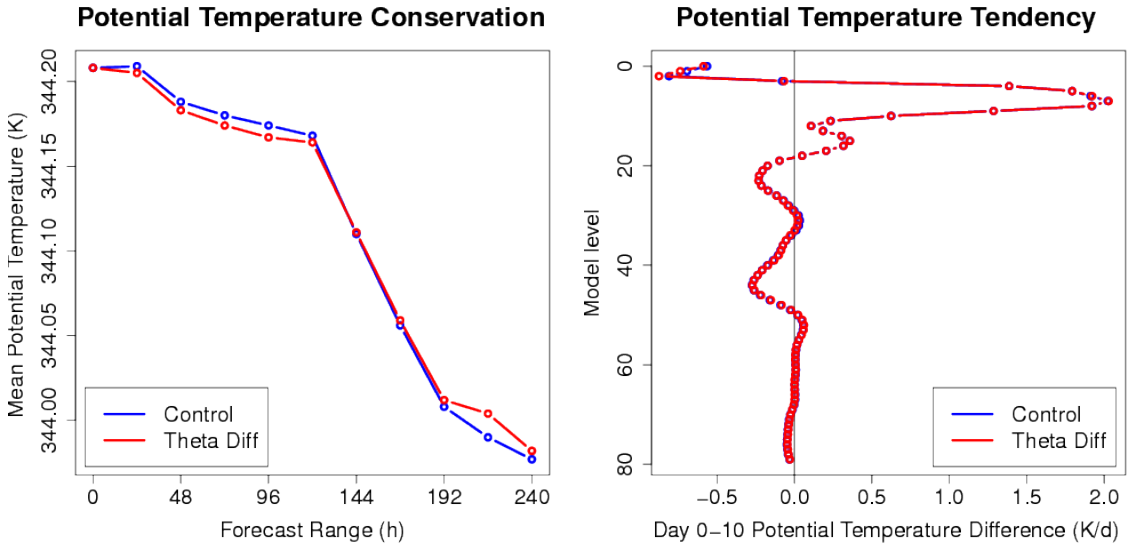

No change to the θ conservation properties of GEM are observed with θ diffusion.

Potential temperature conservation (left, global; right, by level) in a 10-day integration of the parallel 25 km GDPS configuration initialized 1200 UTC 1 Feb 2011 (M. Roch and A. Plante).

Alternate solutions

- Diffusing θ is one solution to the problem of VCP over-cooling:
  - Effective, with minimal impact on guidance
  - Acts on the root cause of the over-cooling problem by preventing the creation of gradients that are too large for the model to resolve
  - A numerical solution to a numerical problem
- Progressive overshoot limiter for R_T:
  - First overshoot at a point is allowed, but the extent of overshooting is progressively limited for each subsequent overshoot at the same point (limits enhanced advective diffusivity)
  - Addresses exactly the root cause of over-cooling (limits side-effects) by eliminating stationary overshoot cooling
  - Expensive conditionals in semi-Lag interpolation
- Parameterized vertical diffusion enhancement
  - Create a “background shear” scaled by subgridscale topographic variability: does not address root cause but might be effective over a broader range of non-numerical VCP errors

Discussion

- A number of problems with near-surface temperatures in GEM-based systems have been fixed in recent years by modifications to horizontal numerical diffusion
- This winter, the operational HRDPS and YEC-15 prototype both experienced VCP over-cooling that led to failures
- The origin of this numerical cooling has been identified to be persistent overshoots in semi-Lagrangian interpolation that occur under a very specific set of topographic and atmospheric conditions
- The solution of θ-diffusion has been introduced in GEM 4.4.3, a process that limits the development of shocks on the grid
- The diffusion of θ appears to be highly effective, although side effects in the HRDPS require study (possibly a second coef)
- Additional solutions are possible and should be discussed

References

Fujita, T. T. and H. A. Brown, 1958: A study of mesosystems and their radar echoes. *Bull. Amer. Meteor. Soc.*, **39**, 538-554.

Haertel, P. T. and R. H. Johnson, 2000: The linear dynamics of squall-line mesohighs and mesolows. *J. Atmos. Sci.*, **57**, 93-107.

Hart, K. A., W. J. Steenburgh, D. J. Onton, and A. J. Siffert, 2004: An evaluation of mesoscale-model-based model output statistics (MOS) during the 2002 Olympic and Paralympic Winter Games. *Wea. Forecasting*, **19**, 200–218.

Johnson, R. H., 2000: Surface mesohighs and mesolows. *Bull. Amer. Meteor. Soc.*, **82**, 13-31.

Reeves, H. D. and D. J. Stensrud, 2009: Synoptic-scale flow and valley cold pool evolution in the western United States. *Wea. Forecasting*, **24**, 1625-1643.

Whiteman, C. D., 1982: Breakup of temperature inversions in deep mountain valleys: Part I. Observations. *J. Appl. Met.*, **21**, 270-289.